学　位　論　文

Type XVII collagen is a deterministic factor of epidermal patterning
（17 型コラーゲンは表皮パターンの決定因子である）

2021 年 03 月

北 海 道 大 学

王 禹楠
Wang Yunan

学　位　論　文

Type XVII collagen is a deterministic factor of epidermal patterning

（17 型コラーゲンは表皮パターンの決定因子である）

2021 年 03 月

北 海 道 大 学

王 禹楠

Wang Yunan

目　　次

発表論文目録および学会発表目録

本研究の一部は以下の論文に投稿中である。

Yunan Wang, Hiroyuki Kitahata, Hideyuki Kosumi, Mika Watanabe, Yu Fujimura, Shota Takashima, Shin-Ichi Osada, Tomonori Hirose, Wataru Nishie, Masaharu Nagayama, Hiroshi Shimizu, Ken Natsuga: Type XVII collagen contributes to epidermal patterning.
Submitted to *Journal of Investigative Dermatology*

本研究の一部は以下の学会で発表した。

Yunan Wang:
HaCaT and DJM-1 Cells Respond Differently to Differentiation Stimulus from Epidermal Keratinocytes.
第 116 回日本皮膚科学会総会 AGORA for Young Asian Dermatologists
2017-06-03 (12:10～12:45)　第 10 会場（仙台国際センター 展示棟会議）

学位論文内容の要旨
(Summary of Dissertation)

博士の専攻分野の名称 博士（医学）　　氏 名 Yunan Wang
（Degree conferred: Doctor of Philosophy）　（Name）

学 位 論 文 題 名（Dissertation Title ）

Type XVII collagen is a deterministic factor of epidermal patterning

17 型コラーゲンは表皮パターンの決定因子である。

【Background and Objectives】Vertebrates exhibit patterned epidermis. In some animals, these are visible through melanin distribution in the skin; in others, they are reflected by the allocation of skin components (e.g. hair follicles and fish scales). Human skin is characterized by fingerprints and similar structures, in which cristae cutis and sulci cutis are found alternately in the epidermis. Although skin patterns have been described in many creatures, the mechanisms underlying the development of these phenotypes are poorly understood. Mouse tail skin serves as a robust model for examining pattern formation, because the epidermis consists of scale (parakeratotic) areas and interscale (orthokeratotic) areas. Tail scale and interscale are distinguished by the expression of keratin 10 (K10) and keratin 31 (K31): scale is K10-/K31+, whereas the interscale epidermis is K10+/K31-. Lineage-tracing experiments have revealed that K10+ interscale epidermis is slow-cycling, whereas K31+ scale areas are fast-cycling.

The epidermis is maintained by the fine-tuned balance between the proliferation and differentiation of epidermal stem cell (SC) progeny. Epidermal SCs need niches to function properly. Integrins (e.g., β1 and α6) and type XVII collagen (COL17) have been implicated as niche proteins for epidermal SCs through colony formation experiments, animal studies, and mathematical modeling. In accordance with this, mice deficient in β1 integrin or COL17 show transient hyperproliferation in the epidermis. Their expression is enriched in human epidermis facing the dermal protrusion but not in the epidermal rete ridges. Interestingly, epidermal scale and interscale areas are not apparent in β1 integrin-null tail epidermis. These previous studies have implicated the involvement of SC niche proteins in the epidermal pattern formation. However, whether these SC niche proteins indeed regulate the epidermal patterns and its underlying mechanisms are unknown.

【Materials and Methods】C57BL/6, *Col17a1*-/-, K14-hCOL17, hCOL17+; *Col17a1*-/-, K5-Cre;*aPKCλ*$^{\Delta E5/\Delta E5}$ (aPKCλ eKO), and *Prkcz*$^{-/-}$ (aPKCζ KO) were used in this study. Tail samples at the mouse age of 4 weeks were obtained after the mice were euthanized. Unstained or stained skin samples were observed by light microscopy or confocal microscopy. Immunofluorescence staining was performed to examine the expression of keratins, COL17 and proliferation markers. When necessary, the obtained images were analyzed by ImageJ software. Quantitative PCR was performed to analyze the keratin gene expression levels. For scale regeneration experiments, the surface of the tail skin was removed by scalpel from C57BL/6 adults. Healed skin samples were obtained 4 to 6 weeks after wounding. Three revertant mosaicism spots and three adjacent diseased skin areas from the upper arm of a junctional epidermolysis bullosa patient were analyzed. The characteristic direction of the epidermal pattern was analyzed by autocorrelation function.

【Results】1) COL17 is preferentially expressed in tail scale epidermis. At P14 and 1-

month-old (1MO), the K31 pattern in the scale epidermis is apparent, and COL17 expression extends to both DEJ and K31-positive suprabasal layers. Suprabasal COL17 is present in the cytoplasm but not in α-catenin-labeled intercellular locations, suggesting that suprabasal COL17 is non-functional and possibly degraded. 2) COL17 deficiency leads to more slender scales in the tail skin. Transgenic rescue by the expression of human COL17 (hCOL17) under the keratin 14 (K14) promoter in *Col17a1*-/- mice reversed the slender scale phenotype. 3) Whole-mount imaging showed that the scale size is smaller in aPKCλ eKO than in littermate controls, but its scale proportion (width/length ratio) is wider than that of controls, which is in contrast to the slender scales of *Col17a1*-/- mice. aPKCζ knockout (aPKCζ KO, *Prkcz*-/-) mice, which have no apparent skin phenotype, showed slightly larger scales, while the width/length ratio did not exhibit significant change. These results show that aPKC deregulation does not phenocopy *Col17a1*-/- scale shape. 4) Expression of wound-induced keratins is pronounced in *Col17a1*-/- tail epidermis. In contrast, normal human epidermal keratinocytes treated with COL17A1 siRNAs did not result in the expression of wound-induced keratins, suggesting that this phenotype is dependent on in vivo settings. 5) Scale shape becomes slender after skin regeneration, and hCOL17 overexpression rescues the phenotype. 6) Taking advantage of the revertant mosaicism in epidermolysis bullosa (EB), in which the mutated genes are corrected spontaneously, COL17-negative (diseased) and COL17-positive (revertant) skin are compared from a junctional EB (JEB) patient with *COL17A1* mutations. The diseased skin surface appears coarse, while the revertant skin is smooth. The autocorrelation functions of the skin images show that the diseased skin harbors a distinct pattern from the revertant skin. These date demonstrate that COL17 influences human skin microtopography.

【Discussion】COL17 is a hemidesmosomal protein that anchors basal keratinocytes to the dermis. As a consequence, COL17 deficiency results in epidermolysis bullosa. Recently, COL17 has also been highlighted as an SC niche protein of hair follicles and epidermis, and its deficiency destabilizes epithelial SC maintenance. Our study provides new insights into COL17 biology. *Col17a1*-/- mice have slender tail scales and are characterized by the expression of wound-induced keratins in the epidermis. In line with this, the regenerated epidermis after wounding shows slender tail scales. hCOL17 overexpression reverses the alteration of scale shapes upon wounding.

Although COL17 interacts with the aPKC complex and helps maintain epidermal cell polarity, *Col17a1*-/- does not exhibit proportionally small scales as seen in aPKCλ eKO mice. This phenotypical difference indicates that the slender scale phenotype in *Col17a1*-/- mice is independent of aberrant cell polarity. The slender scales in *Col17a1*-/- mice most likely represent wound-related skin changes that involve the expression of wound-induced keratins in *Col17a1*-/- epidermis. However, the mechanisms by which wound-related skin changes affect epidermal patterning need further investigation.

Our study has also demonstrated that the presence of COL17 alters human skin microtopography. These facts corroborate the role of COL17 in epidermal patterning and highlight COL17 as a therapeutic target for wound-induced skin deformations.

【Conclusion】Our study suggests that epidermal patterning reflects the behavior of epidermal SCs as well as the cellular cytoskeletal organization, both of which might be altered by dysfunctional niche proteins and minor injury. Our study sheds light on the role of the SC niche in tissue pattern formation. In conclusion, our study highlights the unrecognized role of COL17 in epidermal patterning. We propose that COL17 modulation can be utilized to prevent epidermal deformation upon wounding.

本文中および図中で使用した略語は以下のとおりである。

AP	anterior-posterior
aPKC	atypical protein kinase C
aPKCλ eKO	*aPKCλ*$^{\Delta E5/\Delta E5}$
aPKCζ KO	*Prkcz*$^{-/-}$
COL17	type XVII collagen
DAPI	4’,6-diamidino-2-phenylindole
DEJ	dermo-epidermal junction
EB	epidermolysis bullosa
hCOL17	human COL17
JEB	junctional EB
K6/K16/K17	keratin 6, 16, and 17
K10	keratin 10
K14	keratin 14
K31	keratin 31
LM	lateral-medial
PFA	paraformaldehyde
RT	room temperature
SCs	stem cells
1MO	1-month-old

Introduction

The skin is outermost organ of the body. It protects us from microbes, helps regulate body temperature, and permits the sensations of touch, heat, and cold. Skin is composed of the multilayered epithelium, the epidermis, and the underlying dermis. The epidermis serves as a physical barrier to pathogens and prevents water leakage from the body (Natsuga, 2014). The dermis is tightly connected to the epidermis through basement membrane zone proteins.

The epidermis is maintained by a fine-tuned balance between the proliferation and differentiation of epidermal stem cells (SCs), which reside in the epidermal basal layer (Moreci and Lechler, 2020). In homeostasis, cells lost during turnover will be compensated by cells generated in the basal layer. Basal layer cells give rise to daughter cells that terminally differentiate. During differentiation, the basal cells move upwards to form the spinous layer, the granular layer, and the

outermost cornified layer. Regulation of cell fate is essential in both development and tissue homeostasis. As we mentioned before, to maintain the different tissue lineages that arise from adult stem/progenitor cells, tissues have to balance self-renewal with differentiation through oriented cell division. There have been many studies that provide models of tissue replenishment in the mouse epidermis, in which individual cell divisions give rise to either two daughter cells with identical fate (either both proliferative or committed to differentiate) or different fate in a stochastic manner (Clayton et al., 2007; Doupé et al., 2010; Lim et al., 2013; Mascré et al., 2012; Sada et al., 2016; Sánchez-Danés et al., 2016). This process is regulated by polarity-related proteins. Whereas symmetric cell division (SCD) generates two daughters with similar fate (two progenitors), asymmetric cell division (ACD) produces daughter cells with differential fates (one progenitor and the other differentiated cell). In lower organisms, it is well established

that ACD promotes tissue differentiation, which is essential during development and for tissue homeostasis (Goulas et al., 2012; Knoblich, 2010). In lower organisms the polarity-related protein atypical protein kinase C (aPKC) controls cell fate and ACD by coupling the orientation of the mitotic spindle to the polarized segregation of cell fate determinants (Knoblich, 2010; Lee et al., 2006), resulting in two daughter cells with different fates.

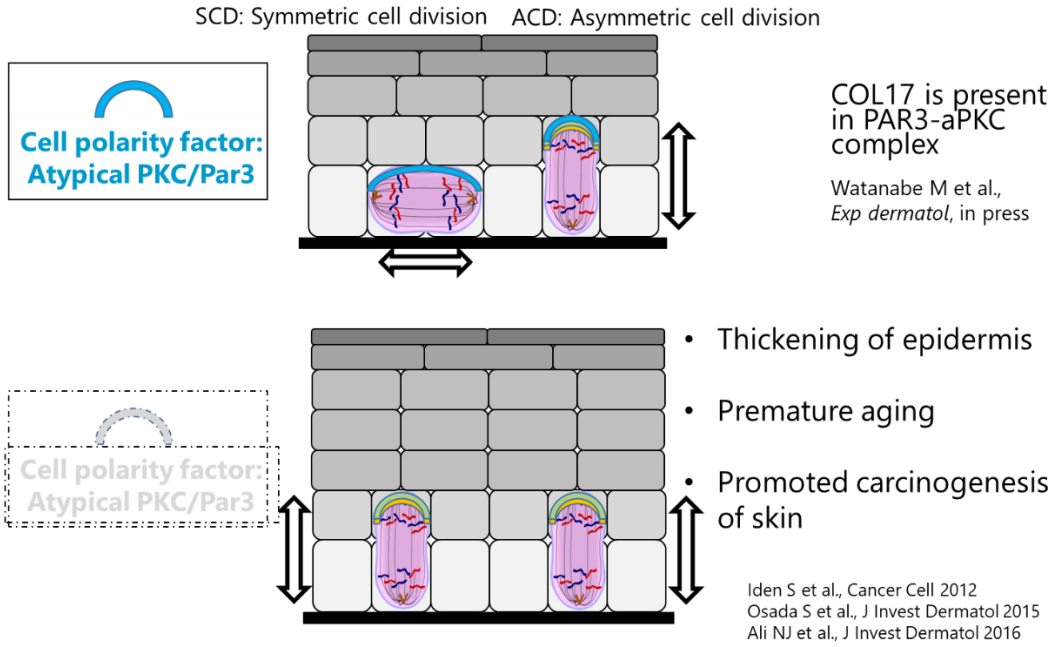

SC niche refers to a microenvironment, which interacts with SCs and fosters their maintenance to regulate cell fate. Epidermal SCs need niche proteins such as integrins and type XVII collagen (COL17) for their proper function (Natsuga et al., 2019; Watt and Fujiwara, 2011). Functional loss of these proteins leads to transient hyperproliferation of the developing epidermis due to disturbed SC maintenance (Brakebusch et al., 2000; Niculescu et al., 2011; Watanabe et al., 2017).

COL17 is a transmembranous protein that is mainly expressed in the epidermal basal keratinocytes. Epidermal-dermal attachment requires COL17 expression at the hemidesmosomes of the epidermal basement membrane zone because congenital COL17 deficiency leads to junctional epidermolysis bullosa and acquired autoimmunity to COL17 induces bullous pemphigoid. Recently, in addition to facilitating epidermal-dermal attachment, COL17 has been reported to serve as a niche for hair follicle SCs, to regulate proliferation in the interfollicular

epidermis (IFE) and to be present along the non-hemidesmosomal plasma membrane of epidermal basal keratinocytes. (Natsuga, 2014)

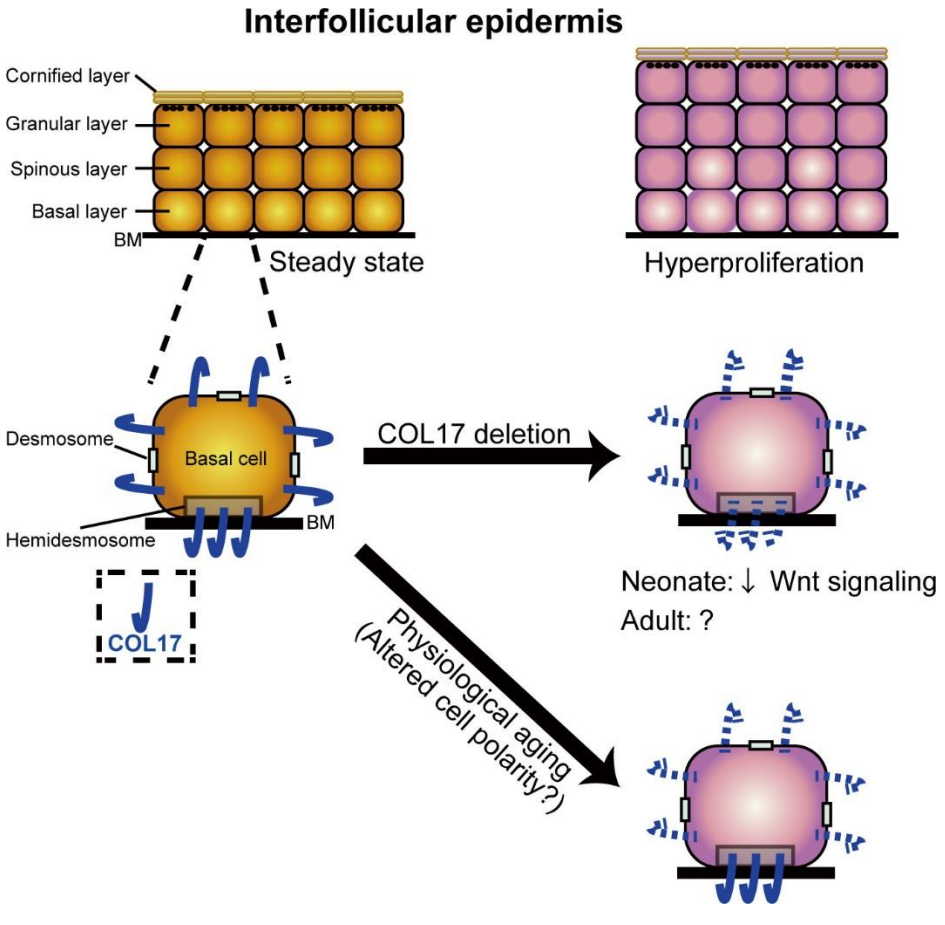

(Natsuga, 2014)

Vertebrates have distinct skin patterns. In some, the patterns are visible through melanin distribution in the skin

(e.g., zebra and tiger stripes); in others, the allocation of skin components forms patterns (e.g., human microtopography, hair follicles, and fish scales). Murine tail skin serves as a robust model for examining epidermal pattern formation (Dekoninck et al., 2020).

In tail epidermis, the hair follicles (HFs) are arranged in groups of three (triplets) in staggered rows (Braun et al., 2003). The IFE adjacent to the HFs is known as the interscale IFE, Interscale IFE undergoes orthokeratotic differentiation, leading to the formation of a granular layer in the outermost viable cell layers and loss of nuclei in the cornified, dead cell layers that cover the surface of the skin. Orthokeratotic differentiation is also characteristic of dorsal IFE. In contrast, tail IFE that is not adjacent to the HFs, known as the

scale IFE, undergoes parakeratotic differentiation characterized by the lack of a granular layer and retention of nuclei in the cornified layers. Scales are regularly spaced and arranged in rows that form rings around the tail. The infundibulum of each HF connects with the interscale IFE while the hair shafts overlie the scales. At birth, the entire tail epidermis is orthokeratotic (Didierjean et al., 1983; Schweizer and Marks, 1977). Scale formation is first detected 9 days after birth (Didierjean et al., 1983; Schweizer and Marks, 1977). From this time point, the tail epidermis consists of scale (parakeratotic) and interscale (orthokeratotic) areas, which are arranged alternately. These scale and interscale areas are distinguished by the expression of keratin 31 (K31) and keratin 10 (K10), respectively (Gomez et al., 2013). Label-retaining and lineage-tracing experiments have revealed that K10+ interscale epidermis is slow-cycling, whereas K31+ scale areas are fast-cycling. Two distinct stem cell populations (Dlx1+ and Slc1a3+) give rise to

interscale and scale epidermis, respectively (Sada et al., 2016), although it is unclear how these cell populations are arranged into scale/interscale patterns.

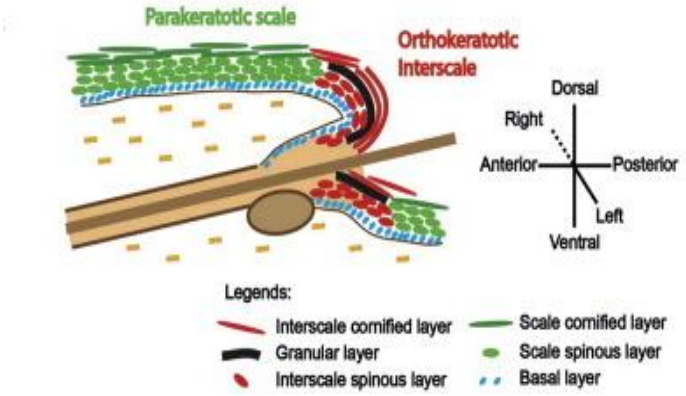

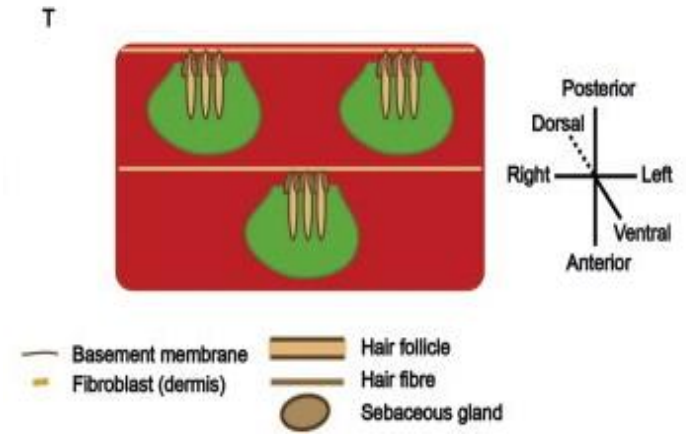

(Gomez et al., 2013)

The expression of epidermal SC niche proteins, including integrins and COL17, shows alternate patterns in the human epidermis, where their expression is enriched in the epidermis facing the dermal protrusion but not in the epidermal rete ridges (Jones et al., 1995; Kobayashi et al., 2018; Wang et al., 2020). Conversely, the scale/interscale patterns are absent in β1 integrin-null tail epidermis (López-Rovira et al., 2005). These previous studies suggest the involvement of SC niche proteins in epidermal pattern formation. However, whether these SC niche proteins indeed regulate the epidermal patterns and the mechanisms underlying such regulation are unknown.

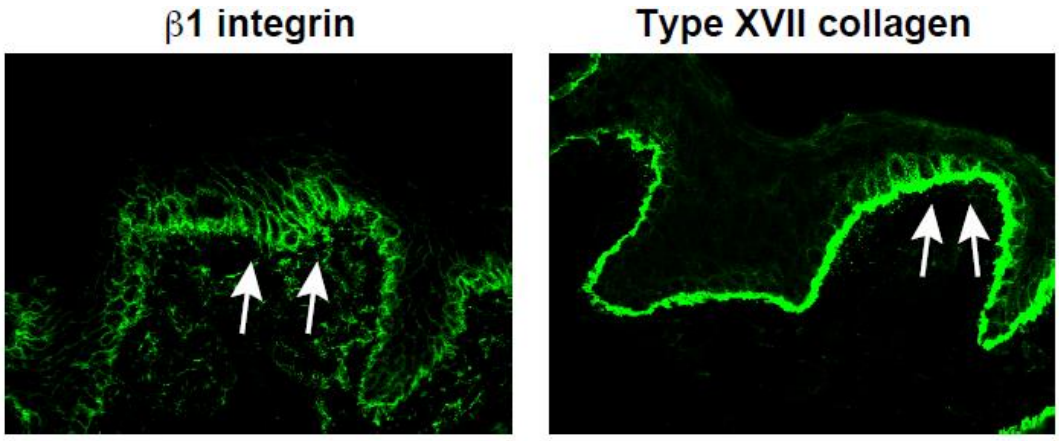

(Kobayashi et al., 2018)

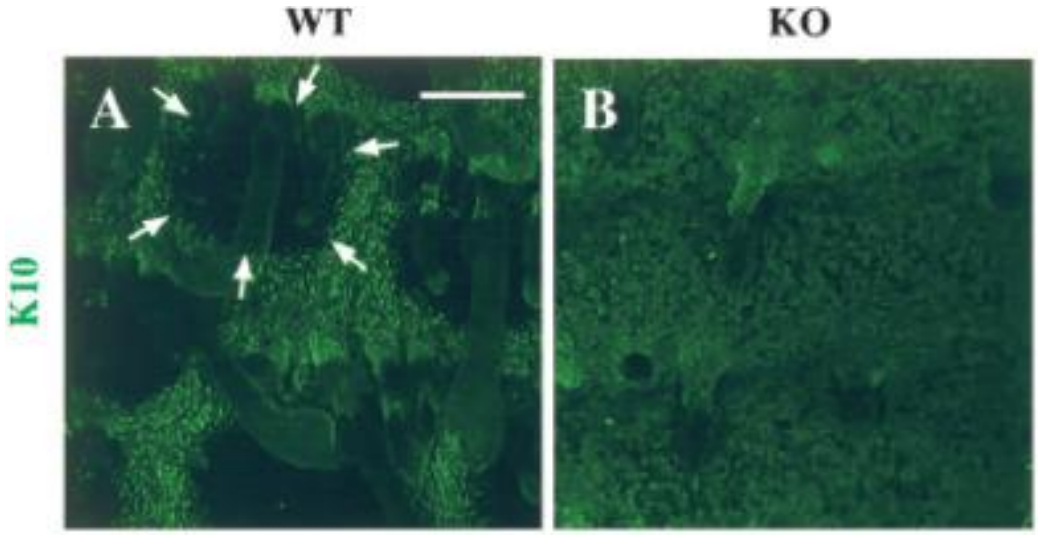

(López-Rovira et al., 2005)

Here, we demonstrate that COL17, an SC niche protein (Liu et al., 2019; Matsumura et al., 2016; Tanimura et al., 2011; Watanabe et al., 2017), helps in the formation of proper epidermal patterns in mice and humans. Interestingly, disturbed epidermal patterning through COL17 deletion is independent of aberrant epidermal cell polarity, but could involve wound-related skin changes.

Material and methods

Animals

C57BL/6 mice were purchased from Clea (Tokyo, Japan). *Col17a1*-/-, K14-hCOL17 (a courtesy gift from Prof. Kim B Yancey), hCOL17+; *Col17a1*-/-, K5-Cre;*aPKCλ*$^{\Delta E5/\Delta E5}$ (aPKCλ eKO), and *Prkcz*$^{-/-}$ (aPKCζ KO) were generated as previously described (Hirate Y et al., Curr Biol 2013; Nishie et al., 2007; Noguchi N et al., J Dermatol Sci 2019; Osada SI et al., J Invest Dermatol 2015). aPKCλ$^{\Delta E5/\Delta E5}$ and *Prkcz*$^{+/-}$ mice were used as aPKCλ eKO and aPKCz KO controls, respectively, and littermate *Col17a1*$^{+/-}$ or *Col17a1*$^{+/+}$ mice were used as *Col17a1*-/- or hCOL17+;*Col17a1*-/- control. The institutional review board of the Hokkaido University Graduate School of Medicine approved all animal studies described below (17-0013).

Genotyping of mice

DNA extraction: Tail samples (5mm) were cut and put into 1.5 ml tube (on ice), followed by incubation with 120 μl of 50 mM NaOH for 30 min at 95℃. 10 μl of 1M Tris-HCl (pH 8.0) was added to the tube and stored at 4℃.

Making agarose gel (2%) for PCR: 4 g of agarose was mixed with 200 ml TBE in conical flask (200 ml). Then the flask was warmed with microwave until the agarose was completely dissolved. Ethidium bromide (10 mg/ml) was added to the conical flask and the agarose solution was poured into a gel tray with well combs.

Genotyping of *Col17a1*-/- mutant mice by PCR. Primers: YA1 (5'-GTGGATTCCCAAAGCCATAC-3'), N1 (5'-TGGATGTGGAATGTGTGCGA-3'), and WT1 (5'-ACCTTCCAGTGAAGAGCCAT-3').

PCR condition: 94℃ 2 min → 98℃ 10 sec, 60℃ 30 sec, 68℃ 45 sec, 35 cycles →68℃ 1 min → 4℃ hold.

Genotyping of hCOL17+ mutant mice by PCR. Primer: B6 (5'-ACCTGGAGTCCCAGGGAAC-3'), F5 (5'- AGACCTGAAGACTGTGTCCA-3').

PCR condition: 94℃ 5 min → 94℃ 1 min, 56℃ 1 min, 72℃ 1 min, 35 cycles→72℃ 7 min → 4℃ hold.

Genotyping of K5-Cre mutant mice by PCR. Primers: K5 Cre-1F (5'-ATGCCAATGCCCCCTCAGTTCCT-3'), K5 Cre-1R (5'-TGCCCCTTTTTATCCCTTCCAGA -3').

PCR condition: 95℃ 3 min → 95℃ 15 sec, 64℃ 15 sec, 72℃ 30 sec, 30 cycles → 72℃ 2 min → 4℃ hold.

Genotyping of *aPKCλ*$^{\Delta E5/\Delta E5}$ (aPKCλ eKO) mutant mice by PCR. Primers: L62 (5'- CATGCAGTGTGCTGGCATAGCCACC-3'), L64 (5'-AGAGGCAGCCAAAGCCCTGCTCTCC -3').

PCR condition: 95℃ 3 min → 95℃ 30 sec, 60℃ 30 sec, 72℃ 45 sec, 30 cycles→72℃ 3 min → 4℃ hold.

Genotyping of *Prkcz*$^{-/-}$ (aPKCζ KO) mutant mice. Primers: Prckz-1 (5'- AAAGGGGCACTGGSGSTTAAACCC-3'), Prckz-2 (5'- GGAATTACCACA CGACCTAGCAGC -3'), Prckz-5 (5'- GCCGTGTGA AATTGTGCTTCAGTG -3').

PCR condition: 95℃ 3 min → 95℃ 30 sec, 60℃ 30 sec, 72℃ 45 sec, 30 cycles → 72℃ 5 min → 4℃ hold.

Antibodies

The following antibodies were used: anti-K31 (Progen, hHa1, Germany), anti-K10 (BioLegend, Poly19054,USA), anti-K6 (BioLegend, Poly19057,USA), anti-α-catenin (α18, provided by Prof. Akira Nagafuchi), anti-cytoplasmic COL17 (Abcam, Cambridge, MA, USA, ab186415; 10C1-1, homemade (Watanabe et al., 2021), and anti-extracellular COL17 (Abcam, ab184996).

Quantitative RT-PCR (qRT-PCR)

RNA was isolated from the tail epidermis or cultured normal human epidermal keratinocytes (NHEKs) using the RNeasy Mini kit (QIAGEN, Hilden, Germany), and cDNA was synthesized using the SuperScript III First-Strand Synthesis System (Thermo Fisher Scientific, Waltham, MA, USA). qRT-PCR was carried out using the designated primers and fast SYBR Green (Thermo Fisher

Scientific) in a STEP-One Plus sequence detection system (Applied Biosystems, Waltham, MA, USA).

The following primers were used for the analysis: Forward primer and reverse primer are: murine *Krt6a*, (5'-CACGTTAAGAAGCAGTGTGCC-3') and (5'-GCTCTGAGCACGGGATTCT-3'); murine *Krt6b*, (5'-AGGAGTGCAGGTTGAATGGTG-3') and (5'-AAAAAGAGAAGCGAGAGGACACA-3'); murine *Krt16*, (5'-TCCCAGCTCAGCATGAAAG-3') and (5'-GAGCTGTGGATATTCTCGCCA-3'); murine *Krt17*, (5'-AGACAGAGAACCGCTACTGC-3') and (5'-CGGGTGGTCACAGGTTCTTTT-3'); murine *Cyc1*, (5'-ATCGTTCGAGCTAGGCATGG-3') and (5'-GCCGGGAAAGTAAGGGTTGA-3'); human *KRT17*, (5'-CAGAGAACCGCTACTGCGTG-3') and (5'-GTCACCGGTTCTTTCTTGTACTG-3'); human *KRT16*, (5'-GCTCAGCATGAAAGCATCCC-3') and (5'-GACCTCGCGGGAAGAATAGG-3'); human *KRT6A*, (5'-AGTGCAGGCTGAATGGCGAA-3') and (5'-TGGGACCGAGAGCTAGCAGA-3'); human *KRT6B*, (5'-TTCATCGACAAGGTGCGGT-3') and (5'-CAGCTCCGAGTCCAGACGAC-3'); human *COL17A1*, (5'-(5'-

(5'-TCAACCAGAGGACGGAGTCA-3') and (5'-TCGACTCCCCTTGAGCAAAC-3'); human *RNA18SN1* (18S), (5'-GGCGCCCCCTCGATGCTCTTAG-3') and (5'-GCTCGGGCCTGCTTTGAACACTCT-3').

Immunofluorescence staining

Paraffin sections were deparaffinized and boiled in citrate or EDTA buffer for 20 min in a microwave oven. Frozen sections were fixed in 4% paraformaldehyde (PFA) for 10 min at room temperature (RT), or cold acetone or used without fixation. After washing with PBS, sections were treated with blocking buffer (0.5% fish skin gelatine, 5% goat serum, 4% BSA in PBS) for 1 h. The samples were incubated with primary antibodies at 4℃ overnight and were subsequently incubated with secondary antibodies conjugated with Alexa fluor 488, Alexa fluor 647, or FITC (1 in 1000) at RT for 1 h. Nuclei were stained with 4',6-diamidino-2-phenylindole (1 in 10000, DAPI). Images were obtained using confocal microscopy (FV1000, Olympus, Tokyo,

Japan; LSM-710, Zeiss, Germany) or fluorescence microscopy (BZ-9000, Keyence, Osaka, Japan).

Whole mount staining

Tail skin was incubated in 5 mM EDTA/PBS on a shaker at 37℃ for 4 h to separate the epidermis from the dermis. Epidermal sheets were fixed in 4% paraformaldehyde (PFA) for 1 h at RT. After blocking, epidermal sheets were incubated with primary antibodies overnight at RT, and then washed in 0.2% Tween/PBS. Samples were subsequently incubated with secondary antibodies. After washing, epidermal sheets were mounted on glass slides in Mowiol solution. The images of whole-mount stained samples were obtained using FV1000 confocal laser scanning microscope (Olympus, Tokyo, Japan) or BZ9000 fluorescence microscope (Keyence, Osaka, Japan). The size and shape of the scales near the midline of the tail epidermis were analyzed using ImageJ (NIH, Bethesda, MD, USA). When the scales of the littermates

were compared, the area, length, and width of the scales were normalized to the whole tail equivalents to exclude the effects of the organismal size of each mouse.

Wound healing experiments

The surface of the tail skin (epidermis and upper dermis, approximately 5 × 4 mm in size) was removed using a scalpel from 1 month-old(MO) C57BL/6 mice. The wounded skin was collected and analyzed when the healing process was complete (typically 4-6 weeks after wounding).

JEB skin analysis

Photographs of the skin of a JEB patient (Nakamura et al., 2006) who was compound heterozygous for c.1179del (p.Ala394Leufs*9) and c.4159C>T (p.Gln1387*) in *COL17A1* (NM_000494.4) were taken by TG-5 (Olympus). Three revertant mosaicism spots and three adjacent diseased skin areas from the upper arm were further

analyzed as described below. The institutional review board of the Hokkaido University Graduate School of Medicine approved all human studies described above (ID: 13-043). The study was conducted according to the principles of the Declaration of Helsinki. The participants provided written informed consent.

Quantification of the skin microtopography

First, the two-dimensional autocorrelation function (right panels in **Figure 18a and 18c**) was calculated for each spot (left panels in **Figure 18a, 18c**). The characteristic direction of the epidermal pattern was detected by determining the direction in which the autocorrelation in the range of a distance less than 1 mm is the largest. The one-dimensional autocorrelation function was calculated (**Figure 18b, 18d**) in the direction perpendicular to the characteristic direction, represented by the red lines in the right panels in Figure 18a and 18c. The peak height (Δ) of the one-dimensional autocorrelation function in the range of

distance less than 1 mm was adopted to quantify the regularity of the pattern. In the case where no peak was detected, the peak height was set to zero.

Statistical analysis

Statistical analysis was performed using GraphPad Prism (GraphPad Software, La Jolla, CA, USA). p-Values were determined using Welch's t-test, Student's t-test, or Mann-Whitney test. p-Values are indicated as *0.01<p<0.05, **0.001<p<0.01, ***0.0001<p<0.001, ****p<0.0001. The values are shown as violin plots.

RESULTS

COL17 is preferentially expressed in tail scale epidermis

We first characterized the distribution of COL17 in C57BL/6 (WT) tail epidermis (**Figure 1**). The K31$^+$ scale epidermis develops at around P2-P9 and matures after P14 (Gomez et al., 2013).

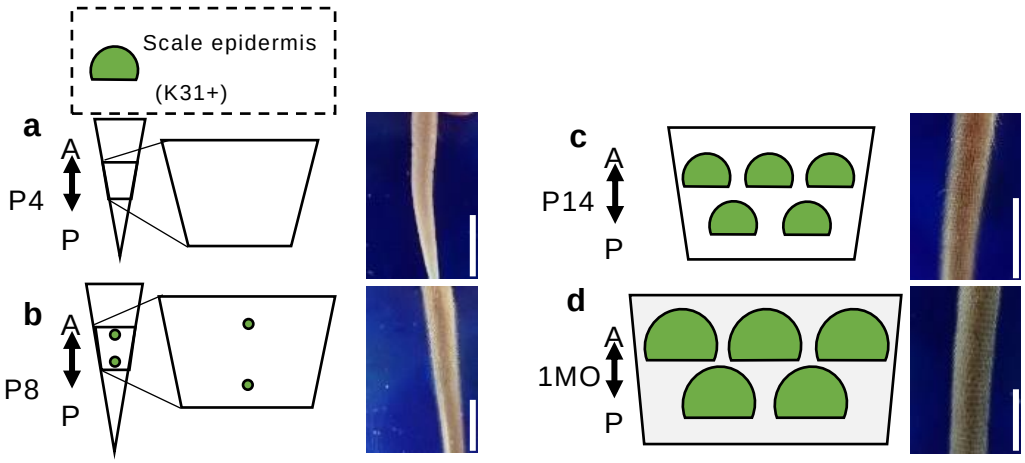

Figure 1. Schematic diagrams of scales (K31$^+$, green) in mouse tail epidermis and representative images of tail skin at P4 (a), P8 (b), P14 (c), and 1-month-old (1MO, d). Scale bar: 5 mm.

Immunofluorescence studies at P4 showed that COL17 expression was confined to the dermo-epidermal junction (DEJ) (**Figure 2**). At P8, when scales were still premature, in addition to COL17 expression at the DEJ, the protein unexpectedly colocalized with K31 in the suprabasal epidermis (**Figure 2, arrowheads**).

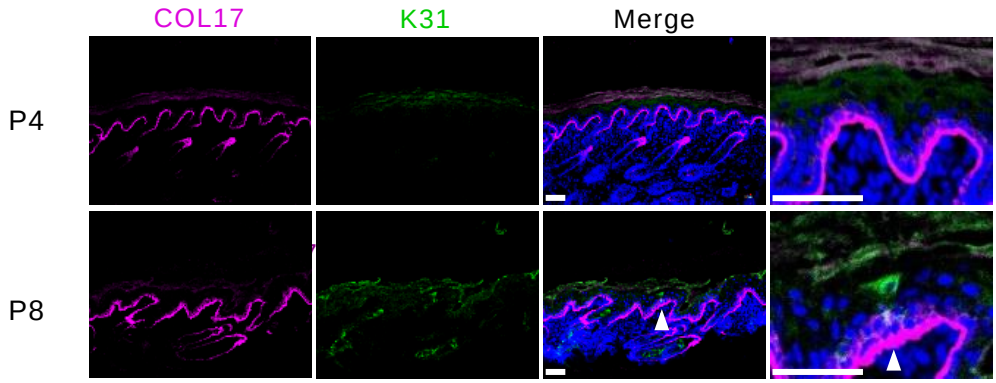

Figure 2. COL17 and K31 staining of tail skin (with DAPI nuclear counterstain) at P4 (n=3), P8 (n=3). Magnified images are shown in the rightmost panels. Scale bar: 60 μm.

At P14 and 1-month-old (1MO), the K31 pattern in the scale epidermis was apparent, and COL17 expression extended to both DEJ and K31-positive suprabasal layers (**Figure 3**).

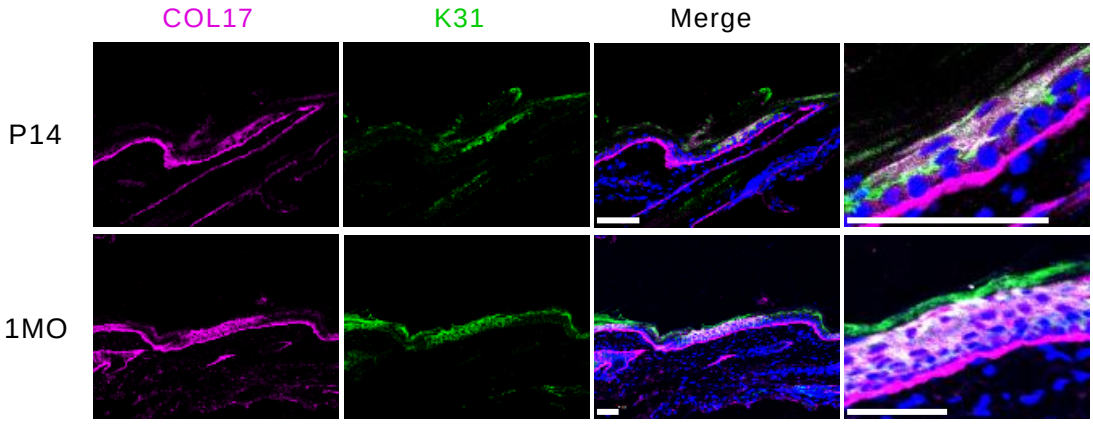

Figure 3. COL17 and K13 staining of tail skin (with DAPI nuclear counterstain) at P14 (n=3), and 1MO (n=4). Magnified images are shown in the rightmost panels. Scale bar: 60 μm.

COL17 enrichment in K31^{+} suprabasal layers was reproduced by multiple COL17 antibodies that react with different regions of the protein (**Figure 4**).

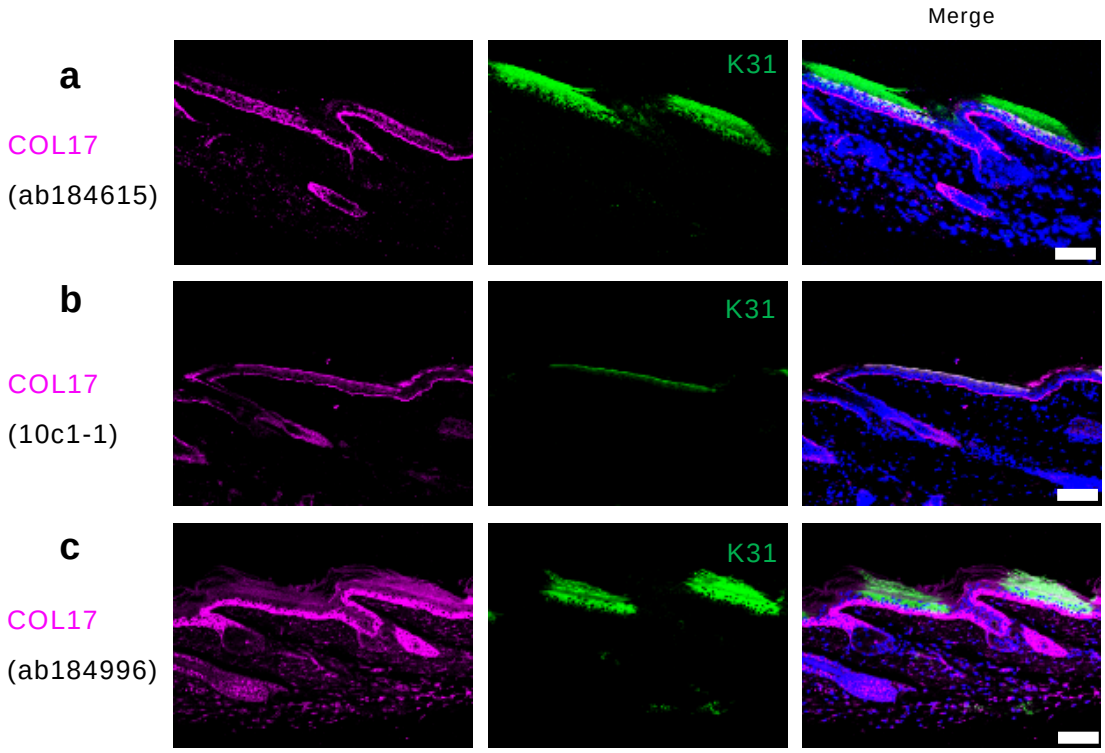

Figure 4. Suprabasal COL17 in tail scale epidermis. (a-c) COL17 and K31 staining of 1MO tail skin. ab186415 (against intracellular COL17, n=4, a), 10C1-1 (against intracellular COL17, n=3, b), and ab184996 (against extracellular COL17, n=3, c) are used. Scale bar: 100 μm.

Suprabasal COL17 was present in the cytoplasm but not in α-catenin-labeled intercellular locations, suggesting that suprabasal COL17 is non-functional and possibly degraded (**Figure**

5). These results show that COL17 marks not only the DEJ but also the K31⁺ suprabasal scale epidermis.

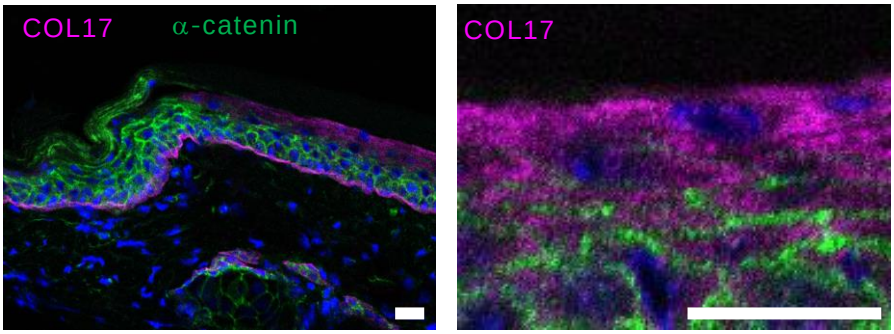

Figure 5. α-catenin and COL17 (ab186415) labeling of 1MO tail skin (n=3). Low- (left) and high-magnified (right, only suprabasal epidermis) images are shown. Scale bar: 20 μm.

COL17 deficiency alters scale shape in the tail skin

We then asked if COL17 is a marker of scale epidermis without any functional significance or it is involved in the scale/interscale patterning of the epidermis. To investigate this, we analyzed tail skin samples of *Col17a1*-/- mice (Nishie et al., 2007) at 1MO when the scales became mature (Dekoninck et al., 2020)

Immunofluorescence of the tail sections showed K10⁺ interscale and K31⁺ scale alternate patterns in both *Col17a1*-/- and controls (**Figure 6**).

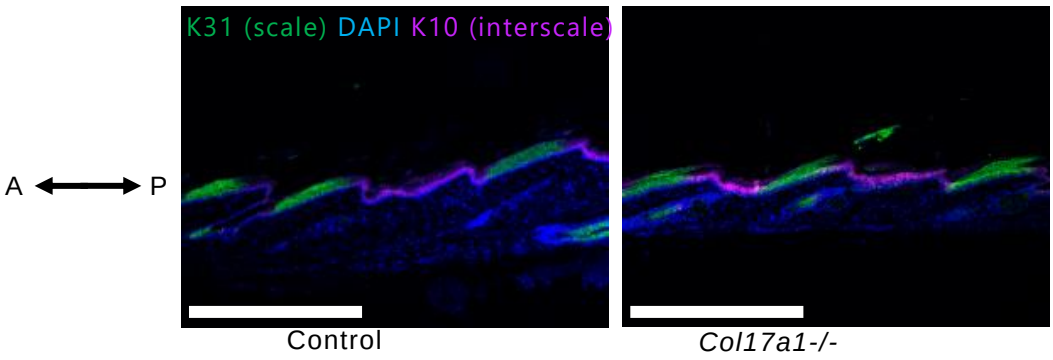

Figure 6. Images showing K31 and K10 staining of Col17a1-/- and control tail skin samples at 1MO (n=4). Scale bar: 500 μm.

We further examined the scale shape by whole skin imaging. We defined the length and width of a scale as the diameter of the anterior-posterior (AP) and lateral-medial (LM) axes, respectively (**Figure 7**). Whole-mount imaging showed that the scale size was smaller and the shape was more slender (shorter on the LM axis) in the *Col17a1*-/- tail epidermis than in the littermate controls (**Figure 7c-7f**).

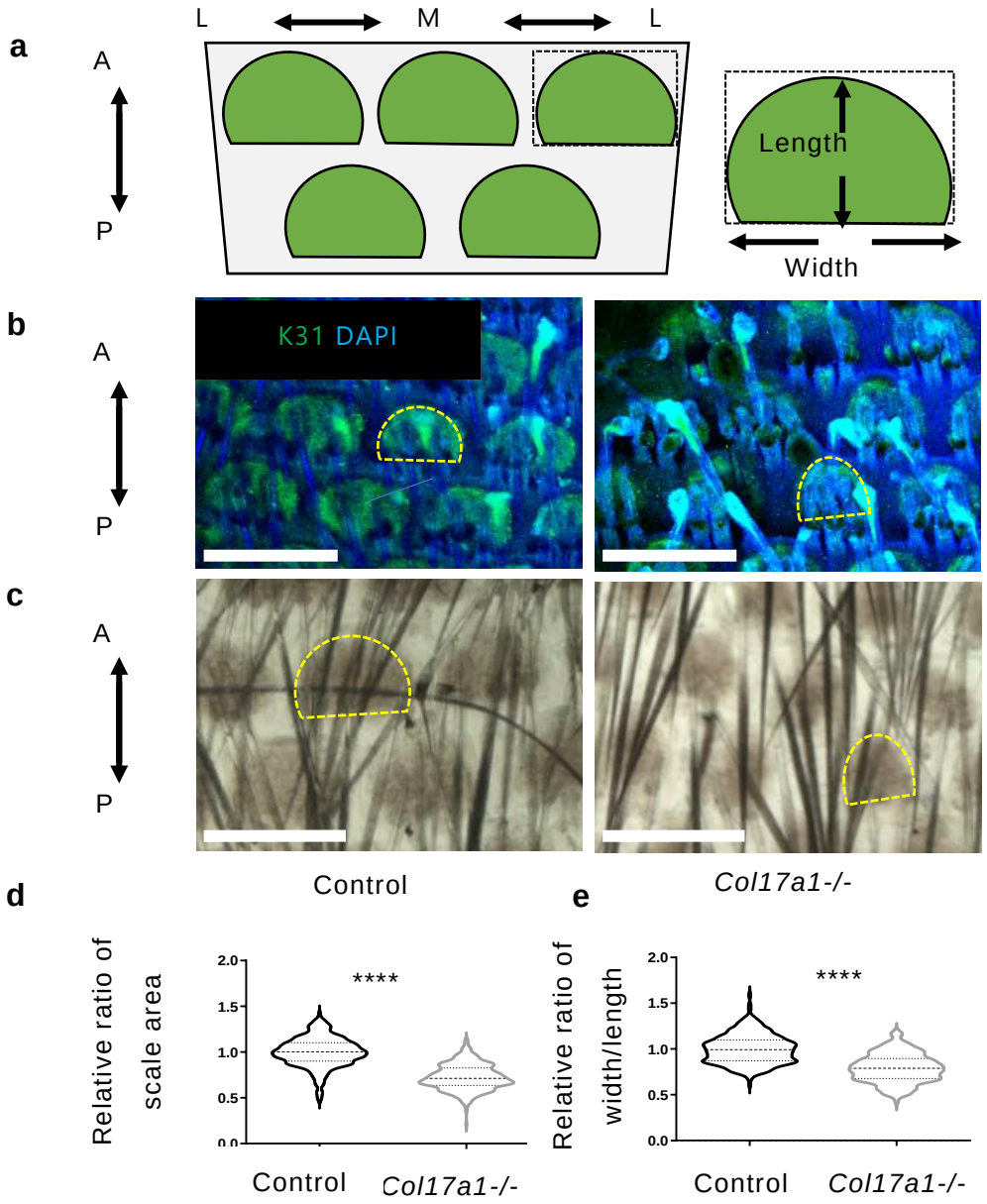

Figure 7. (a) Schematic of distribution of scales in mouse tail epidermis. (b) K31 whole mount staining images of *Col17a1*-/- and littermate control tail epidermis at 1MO (n=3). Scale bar: 500 μm. (c) Phase-contrast images of *Col17a1*-/- and littermate control tail epidermis at 1MO (n=4). Scale bar: 500 μm. (d-e) Quantification of the size and shape of tail scales. Scale area (d) and width/length (e) of *Col17a1*-/- and littermate control tail scales at 1MO are shown (n=298 scales from three control and 413 scales from three *Col17a1*-/- mice).

The shorter scale width in *Col17a1*-/- explains the smaller size of *Col17a1*-/- scales because their length was comparable to that of the controls (**Figure 8a, 8b**) As the WT scale shape was wider at P14 than at 1MO (**Figure 8c**), the slender scale shape in *Col17a1*-/- mice was not due to the delayed development of the mice.

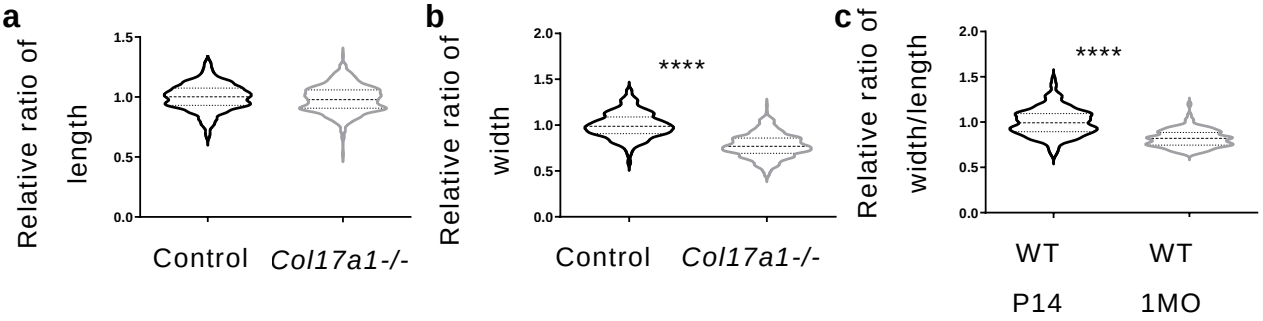

Figure 8. Quantification of the size and shape of tail scales. Length (a), and width (b) of *Col17a1*-/- and littermate control tail scales at 1MO are shown (n=298 scales from three control and 413 scales from three *Col17a1*-/- mice). (c) Width/length ratio of tail scales in P14 and 1MO WT mice (n=148 scales from three P14 WT mice and 123 scales from three 1MO WT mice).

Transgenic rescue by the expression of human COL17 (hCOL17) under the keratin 14 (K14) promoter in *Col17a1*-/- mice (Nishie et al., 2007) reversed the slender scale phenotype (**Figure 9**). These data indicate that COL17 helps to define the scale proportion.

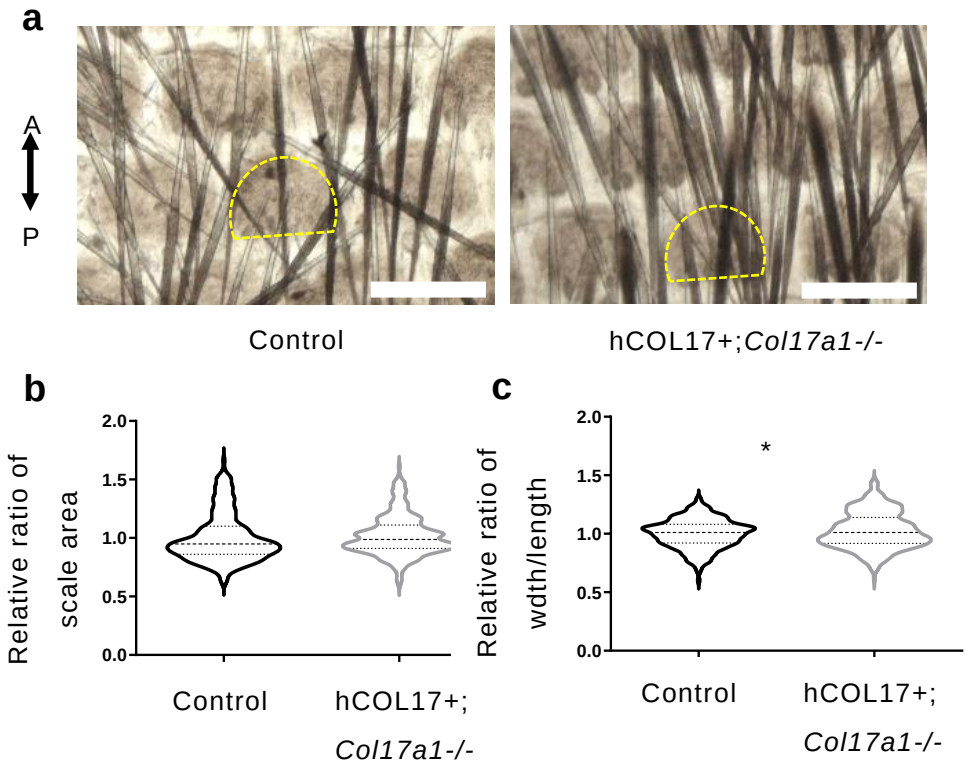

Figure 9. (a) Whole mount phase-contrast imaging of hCOL17+; *Col17a1*-/- and littermate control (hCOL17-; *Col17a1*+/+ or hCOL17-;*Col17a1*+/-) tail epidermis at 1MO (n=3). Scale bar: 500 μm. (b, c) Quantification of the size and shape of tail scales. Scale area (b) and width/length (c) of hCOL17+; *Col17a1*-/- and littermate control tail scales at 1MO are shown (n=266 scales from three control and 359 scales from three hCOL17+;*Col17a1*-/- mice). *0.01<p<0.05, Welch's t-test.

aPKC deregulation does not phenocopy *Col17a1*-/- scale shape

Atypical protein kinase C (aPKC) is a key regulator of epithelial polarity (Niessen et al., 2013), and the epidermis expresses two aPKC isoforms (aPKCλ and aPKCζ) (Helfrich et al.,

2007). The ablation of aPKCλ in the epidermis (K5-Cre; *aPKCλ*$^{\Delta E5/\Delta E5}$, aPKCλ eKO) and *Col17a1*-/- mice share premature aging phenotypes such as gray hair and hair loss (Niessen et al., 2013; Nishie et al., 2007; Osada et al., 2015; Tanimura et al., 2011). This phenotypic similarity has been proposed to be a consequence of the interaction between COL17 and the aPKC complex (Watanabe et al., 2021). We asked if the destabilized aPKC accounts for the slender scale shape of *Col17a1*-/- mice (**Figure 10, 11**).

Whole-mount imaging showed that the scale size was smaller in aPKCλ eKO than in littermate controls, but its scale proportion (width/length ratio) was wider than that of controls (**Figure 10a, 10b, 10c**), which is in contrast to the slender scales of *Col17a1*-/- mice (**Figure 7**).

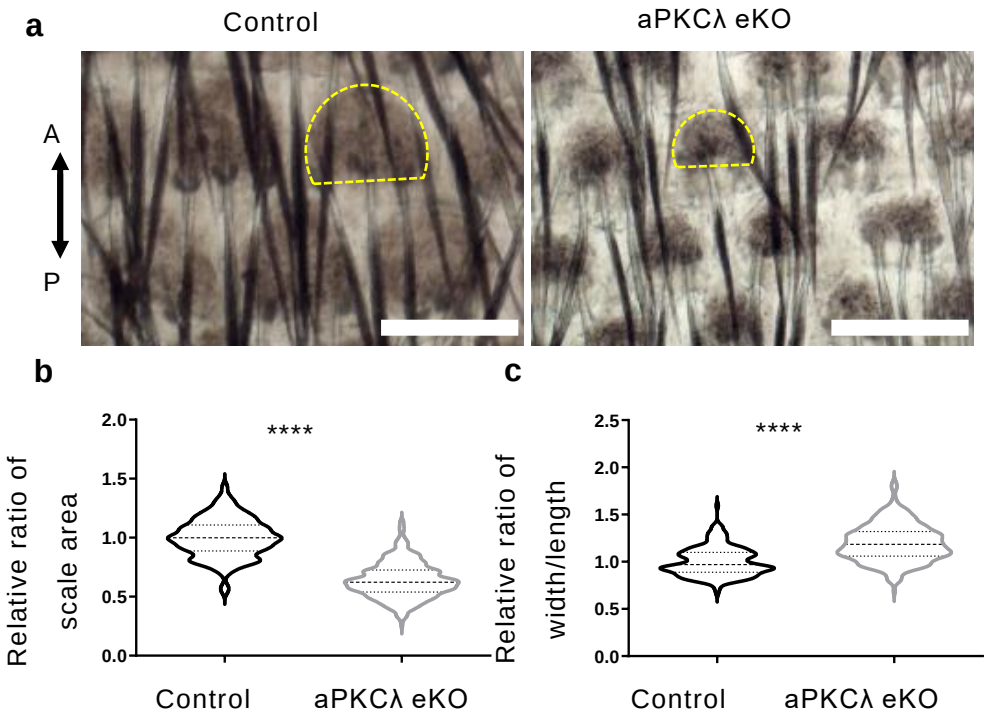

Figure 10. (a) Whole mount phase-contrast imaging of aPKCλ eKO and littermate control tail epidermis (n=3). Scale bar: 500 μm. (b-c) Quantification of the size and shape of tail scales. Scale area and width/length of aPKCλ eKO tail scales at 1MO are shown (n=226 scales from three control mice and 357 scales from three aPKCλ eKO mice, ****$p<0.0001$, *$0.01<p<0.05$, Welch's t-test.

aPKCζ knockout (aPKCζ KO, *Prkcz*-/-) mice, which have no apparent skin phenotype (Noguchi et al., 2019), showed slightly larger scales, while the width/length ratio did not exhibit significant change (**Figure 11**). These results indicate that the aberrant cell polarity in *Col17a1*-/- epidermis (Liu et al.,

2019; Watanabe et al., 2021) is not involved in altering the scale shape.

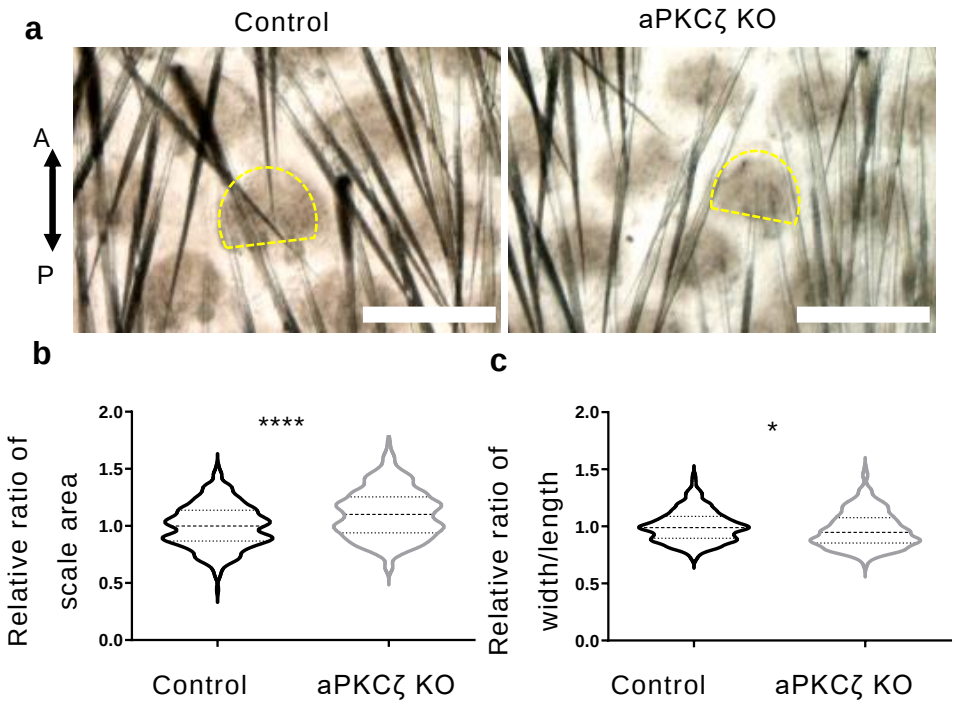

Figure 11. (a) Whole mount phase-contrast imaging of aPKCζ KO and littermate control tail epidermis (n=3). Scale bar: 500 μm. (c-f) Quantification of the size and shape of tail scales. Scale area and width/length of aPKCζ KO (b, c) tail scales at 1MO are shown (n=300 scales from three control mice and 317 scales from three aPKCζ KO mice). ****$p<0.0001$, *$0.01<p<0.05$, Welch's t-test.

Expression of wound-induced keratins is pronounced in *Col17a1*-/- tail epidermis

One of the factors that may affect scale shape is the cytoskeleton of epidermal keratinocytes. Keratin 6, 16, and 17 (K6/K16/K17) are the well-known keratins expressed upon physical injury. We reasoned that these wound-induced keratins might be enriched in *Col17a1*-/- epidermis at steady state because COL17 deficiency leads to epidermolysis bullosa in humans (McGrath et al., 1995) and shows skin fragility in mice (Nishie et al., 2007).

Quantitative PCR revealed that the gene expression of these wound-induced keratins was higher in *Col17a1*-/- tail epidermis (**Figure 12**).

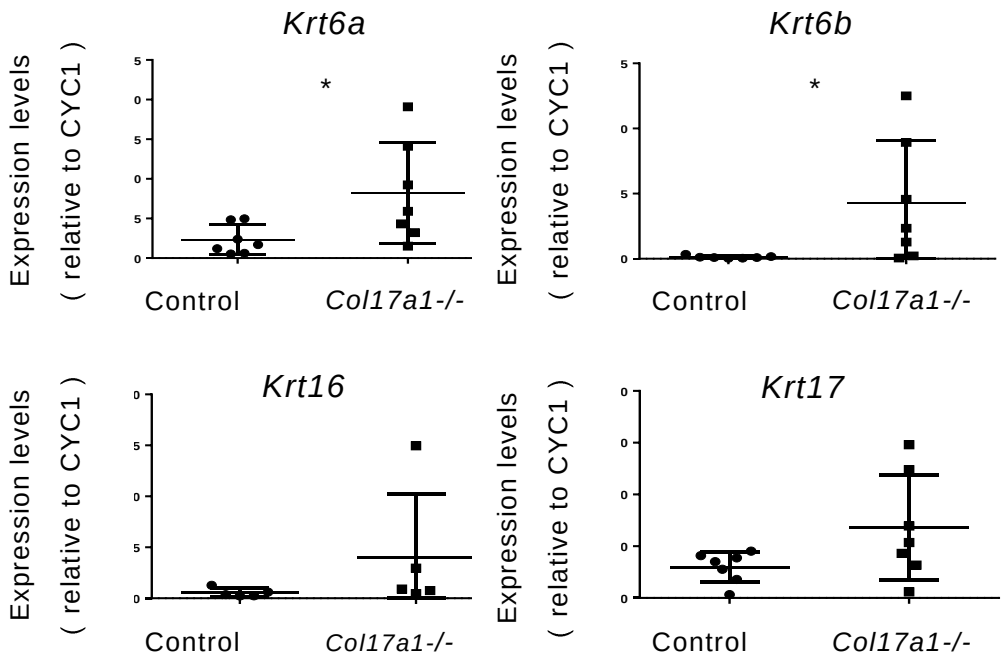

Figure 12. Gene expression of *Krt6a*, *Krt6b*, *Krt16*, and *Krt17* in the tail epidermis of *Col17a1*-/- and littermate control at 1MO (n = 7). *0.01<p<0.05, Student's t-test.

In addition to gene expression, immunofluorescence analyses showed ectopic K6 expression in *Col17a1*-/- tail epidermis at 1MO. K6 expression in *Col17a1*-/- tail epidermis was also observed during the developmental stages (P1 and P14; **Figure 13a-13b**). These data indicate that keratin profiles are skewed towards the wound-induced subsets in *Col17a1*-/- epidermis.

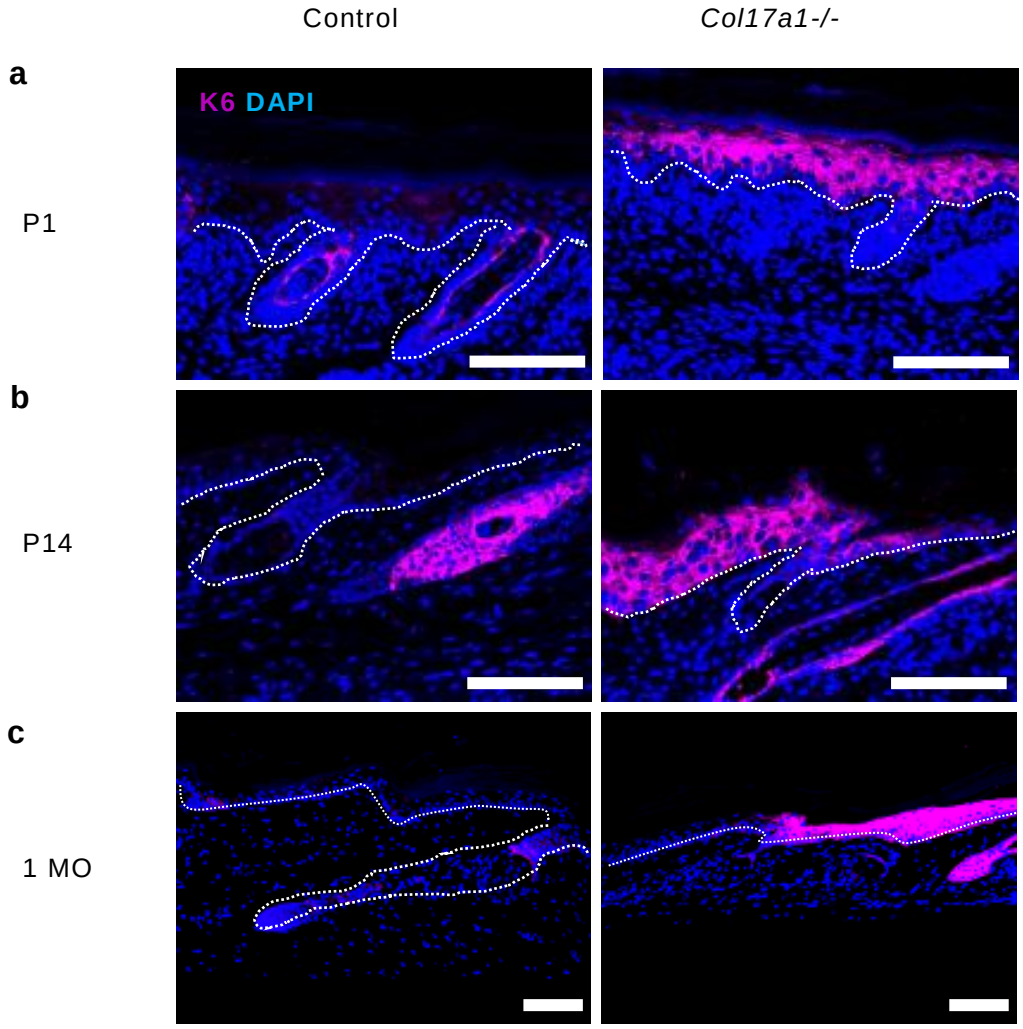

Figure 13. (a-c) K6 staining of *Col17a1*-/- and littermate control at P1 (a, n = 3), P14 (b, n = 3), and 1MO (c, n = 3). Scale bar: 100 μm.

In contrast, normal human epidermal keratinocytes treated with *COL17A1* siRNAs did not result in the expression of wound-induced keratins (**Figure 14**), suggesting that this phenotype is dependent on *in vivo* settings.

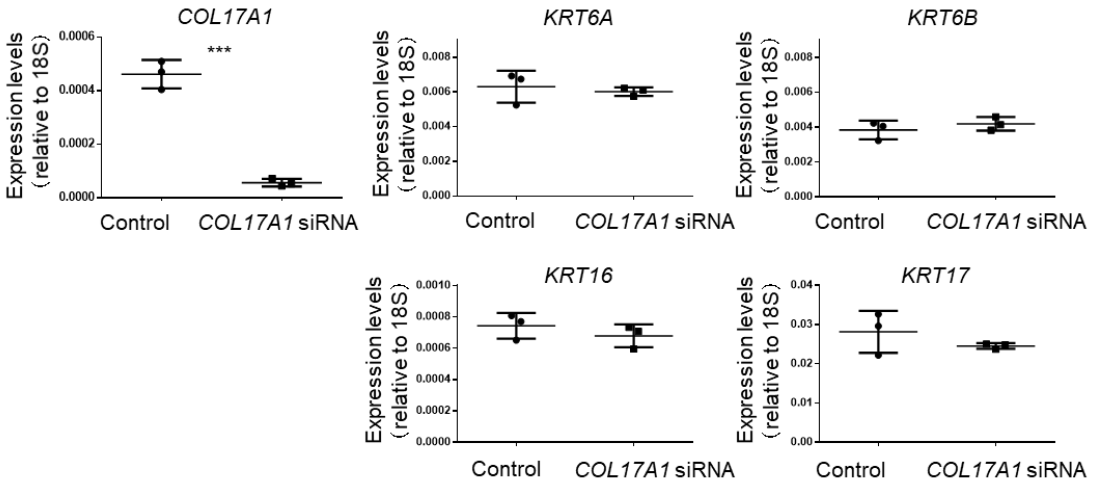

Figure 14. COL17A1 knockdown on normal human epidermal keratinocytes (NHEKs). Expression of COL17A1, KRT6A, KRT6B, KRT16, and KRT17 in NHEKs treated with COL17A1 siRNA or mock (n=3). ***p<0.0001.

Scale shape becomes slender after skin regeneration, and COL17 overexpression rescues the phenotype

The expression of wound-induced keratins in *Col17a1*-/- epidermis led us to ask whether wounding itself alters the tail scale shape upon skin regeneration (**Figures 15-16**). The regenerated tail epidermis (4 to 6 weeks after wounding) exhibited a more

slender scale shape than the non-lesional areas (**Figure 15a, 15b, 15c**), recapitulating the *Col17a1*-/- scale (**Figure 7**).

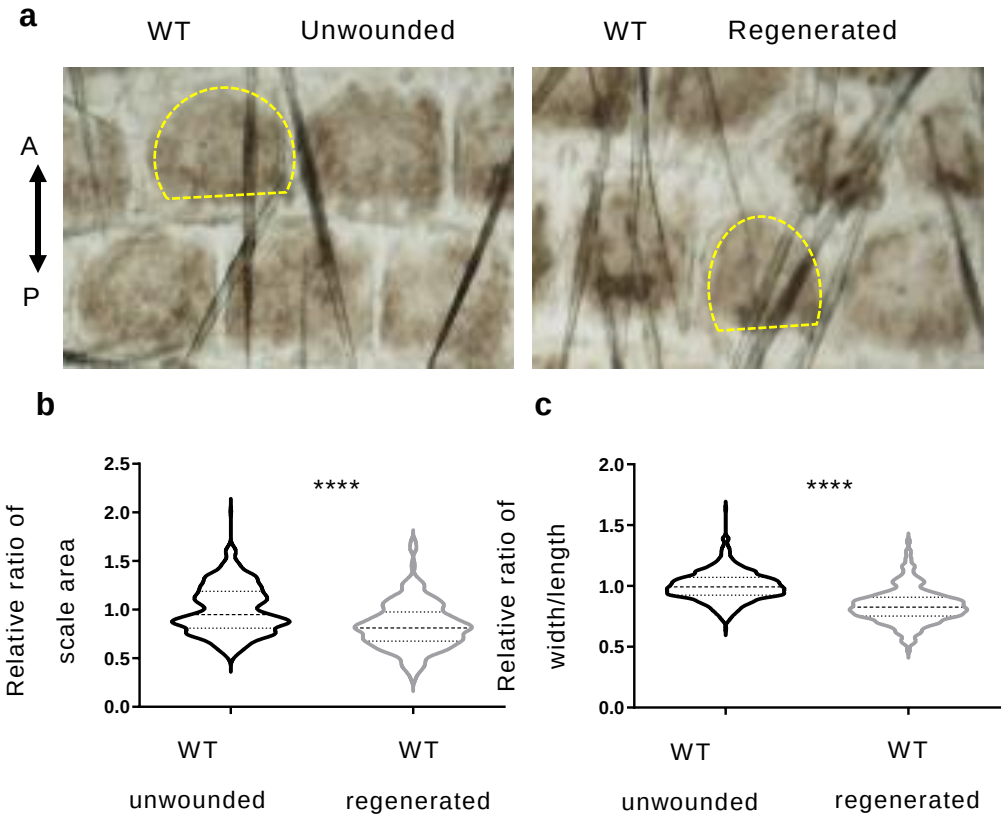

Figure 15. (a) Whole mount phase-contrast imaging of WT tail epidermis after skin regeneration (n=3). Scale bar: 500 μm. (b-c) Quantification of the size and shape of tail scales. Scale area and width/length of WT tail scales after skin regeneration are shown (n=542 scales from three unwounded areas, and 467 scales from three regenerated areas from four WT mice). ****p<0.0001, Welch's t-test.

To see that additive COL17 prevents the alteration of the scale shape in the regenerated epidermis, we utilized K14-hCOL17 transgenic mice, which overexpress hCOL17 under the K14 promoter. The scale shape of the regenerated K14-hCOL17 skin was not as slender as that of the regenerated WT skin (**Figure 15**). These results suggest that COL17 prevents wound-induced scale deformation.

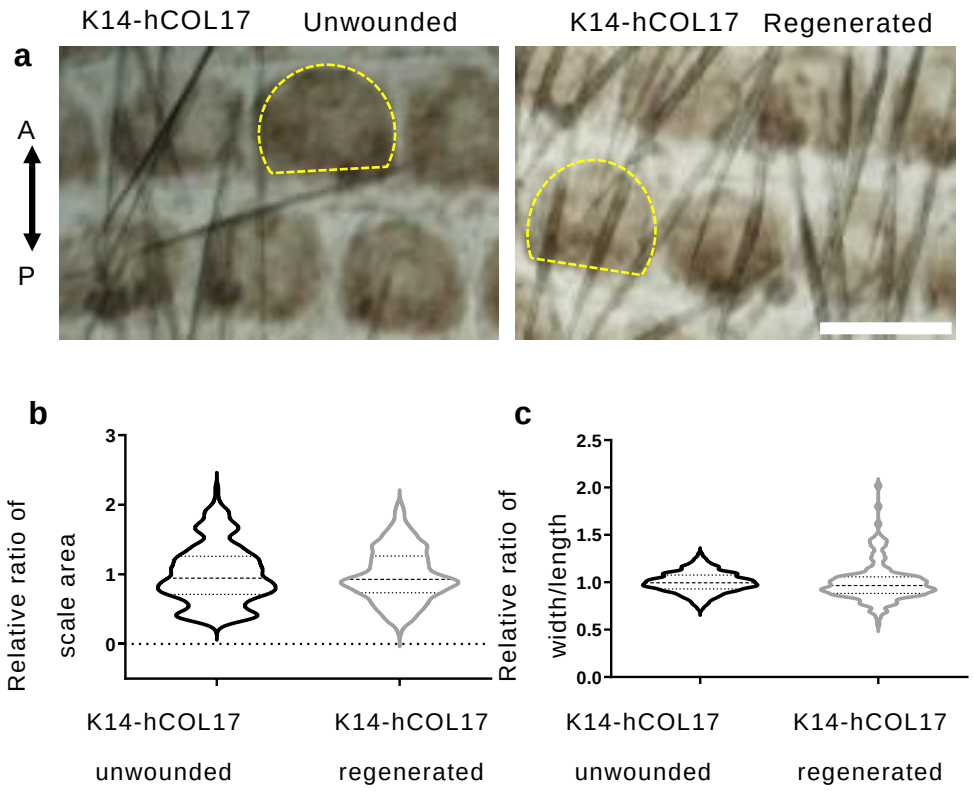

Figure 16. (a) Whole mount phase-contrast imaging of K14-hCOL17 tail epidermis after skin regeneration (n=3). Scale bar: 500 μm. (b-c) Quantification of the size and shape of tail scales. Scale area and width/length of K14-hCOL17 tail scales after skin regeneration are shown (n=424 scales from three control mice and 440 scales from six K14-hCOL17 mice).

COL17 influences human skin microtopography

We finally asked whether the presence or absence of COL17 also affects epidermal patterning in humans. Although scale/interscale epidermal patterns in mouse tails are not conserved, skin surface patterns consisting of grooves and ridges are visible in humans. We took advantage of the revertant mosaicism in epidermolysis bullosa (EB), in which the mutated genes are corrected spontaneously (Jonkman and Pasmooij, 2009; Nomura, 2020).

We compared COL17-negative (diseased) and COL17-positive (revertant) skin from a junctional EB (JEB) patient with *COL17A1* mutations (Nakamura et al., 2006) (**Figure 17a-17c**). The diseased skin surface appeared coarse, while the revertant skin was smooth (**Figure 17b**).

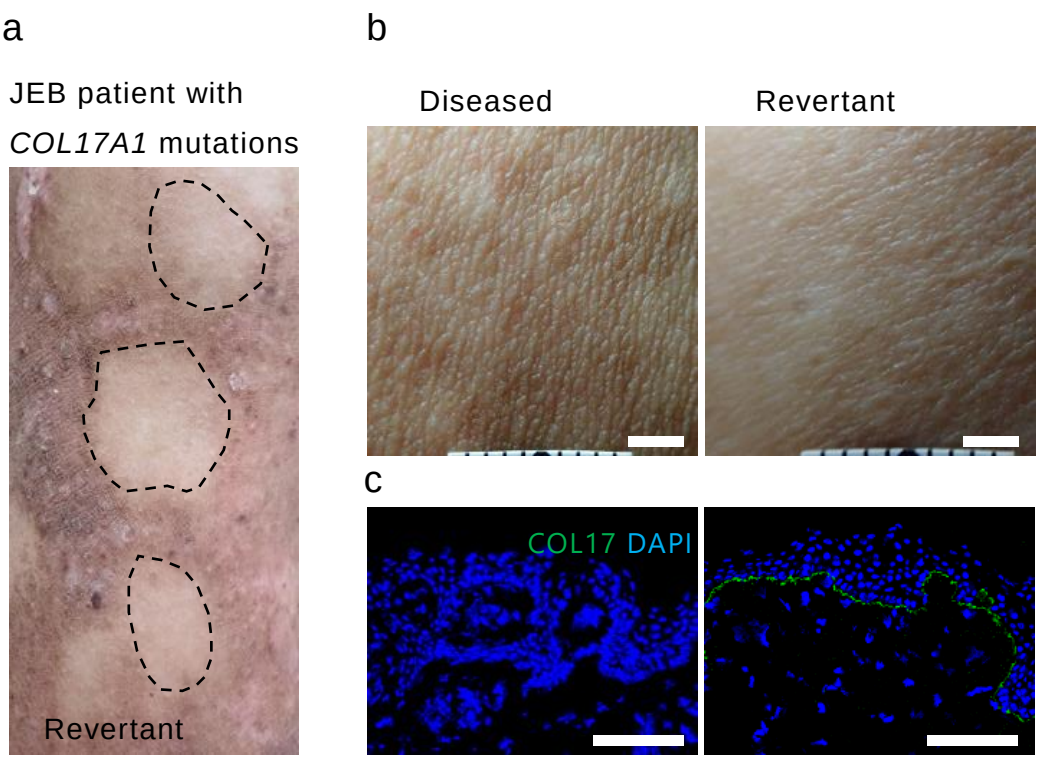

Figure 17. (a) The upper arm of a junctional epidermolysis bullosa patient who is compound heterozygous for c.1179del (p.Ala394Leufs*9) and c.4159C>T (p.Gln1387*) in *COL17A1* (NM_000494.4). The revertant skin areas are circled by dotted lines. (b) Representative images of the diseased and revertant skin. Scale bar: 3 mm. (c) COL17 labeling of the diseased and revertant skin. Scale bar: 100 μm.

We calculated the autocorrelation functions of these skin images to quantify the skin microtopography and found that the diseased skin shows a distinct pattern from the revertant skin (**Figure 18a-e**). These findings demonstrate that COL17 is a deterministic factor of epidermal patterning in mice and humans.

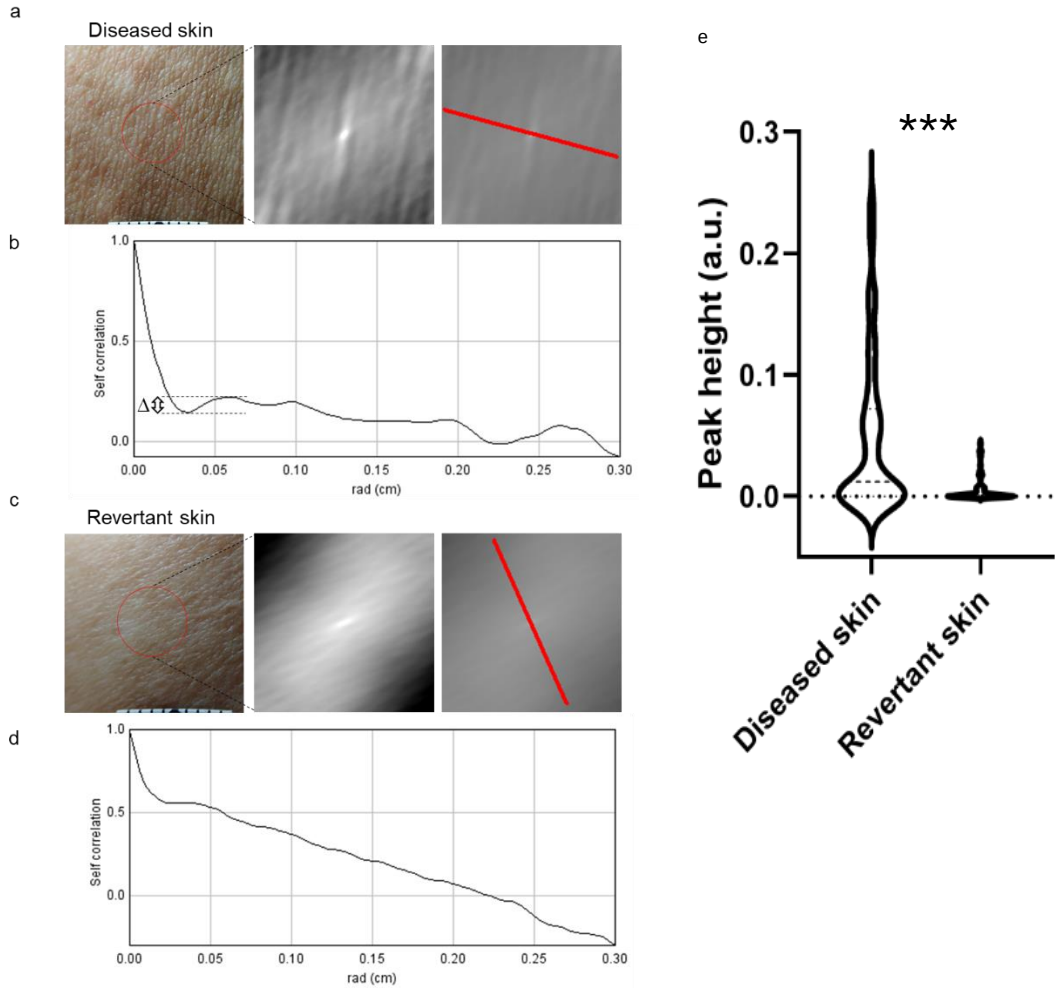

Figure 18. (a, c) The position of the spot with a radius of 3 mm for quantification. The two-dimensional autocorrelation function for the epidermal pattern with the red line perpendicular to the characteristic direction. The one-dimensional autocorrelation is calculated along the line for the diseased (a) and revertant (c) skin. Scale bars: 3 mm (left) and 1 mm (right). (b, d) One-dimensional autocorrelation function in the diseased skin (b) and the revertant skin (d). The peak height (Δ) is defined as the difference between the first local minimum and local maximum in the range of the distance less than 1 mm (e) Quantification of skin microtopography (n=75 spots (radius: 3 mm) from three skin areas, respectively). The degree of regularity on the epidermal pattern was quantified by the peak height of the autocorrelation function (a-d). ***0.0001<p<0.001, Mann-Whitney test.

Discussion

COL17 is a hemidesmosomal protein that anchors basal keratinocytes to the dermis. COL17 stabilizes hemidesmosomes by binding to various basement membrane zone proteins including BP230 (Hopkinson and Jones, 2000; Koster et al., 2003), α6 integrin (Hopkinson et al., 1995), β4 integrin (Aho and Uitto, 1998; Hamill et al., 2011; Koster et al., 2003; Schaapveld et al., 1998), plectin (Koster et al., 2003; Natsuga et al., 2017), laminin-332 (Nishimura et al., 2016; Tasanen et al., 2004), and type IV collagen (Kamaguchi and Iwata, 2019; Nishie et al., 2011).As a consequence, COL17 deficiency results in epidermolysis bullosa (McGrath et al., 1995; Nishie et al., 2007). Recently, COL17 has also been highlighted as an SC niche protein of hair follicles and epidermis, and its deficiency destabilizes epithelial SC maintenance (Liu et al., 2019; Matsumura et al., 2016; Tanimura et al., 2011; Watanabe et al., 2017).

Epidermal cell polarity regulates symmetrical and asymmetrical cell division of basal keratinocytes (Morrow et al., 2019; Muroyama and Lechler, 2012; Poulson and Lechler, 2012) and is regulated by the aPKC complex (Niessen et al., 2012; Tellkamp et al., 2014; Vorhagen and Niessen, 2014). Increased asymmetrical cell division in aPKCλ eKO epidermis (Niessen et al., 2013) and possible stem cell depletion explain the smaller scales in aPKCλ eKO mice (**Figure 10**). Although COL17 interacts with the aPKC complex (Watanabe et al., 2021) and helps maintain epidermal cell polarity (Liu et al., 2019; Watanabe et al., 2021), *Col17a1*-/- did not exhibit proportionally small scales as seen in aPKCλ eKO mice. This phenotypical difference indicates that the slender scale phenotype in *Col17a1*-/- mice is independent of aberrant cell polarity.

There are several aspects of polarization in different cell types and tissues. In addition to the ubiquitous epithelial cell

polarity along the apical-basolateral axis, many epithelial tissues and organs are also polarized within the plane of the epithelium. This is generally referred to as planar cell polarity (PCP; or historically, tissue polarity). PCP is not restricted only to epithelial tissues but is also found in mesenchymal cells, where it can regulate cell migration and cell intercalation. Moreover, particularly in vertebrates, the conserved core PCP signaling factors are associated with the orientation or formation of cilia. (Simons and Mlodzik, 2008)(Matias Simons and Marek Mlodzik Rev. Genet. 2008). We are wondering if the PCP of the epidermal basal cells could account for the slender scale phenotype of Col17a1-/- mice. We are going to determine the cell division direction in the plane of scale basal cell layers in Col17a1-/- tail skin and hCOL17+; Col17a1-/- tail skin by using survivin/keratin 14 staining. Through these analyses, we would be able to see whether the altered PCP could explain the Col17a1-/- phenotype, in that cell division

along A-P axis rather than L-M axis might be pronounced in Col17a1-/- compared with control mice.

Among various skin patterns, fingerprints, also called dermatoglyphics, are the most well-characterized in humans. Fingerprints show an alternate pattern of epidermal ridges and grooves. Loss of fingerprints has been described in EB patients, including Kindler syndrome (Almeida et al., 2015; Has et al., 2010) and junctional EB with *COL17A1* p.Arg1303Gln mutation (Nishimura et al., 2016; Stouthamer et al., 2001; Yuen and Jonkman, 2011). Our study has also demonstrated that the presence of COL17 alters human skin microtopography (**Figure 17**). These facts corroborate the role of COL17 in epidermal patterning and highlight COL17 as a therapeutic target for wound-induced skin deformations.

To further confirm the role of COL17 in the epidermal patterning, it is plausible to look into Col17 knock-down zebrafish skin (Kim et al., 2010) Unfortunately, the skin

pattern of the Col17 knock-down zebrafish has not been investigated. This is partly because the zebrafish injected either with col17a1a or col17a1b morpholinos die at 6-8 days after birth (Kim et al., 2010).

Hemidesmosomes are complex junctions that anchor epithelial cells to the basement membrane and are composed of adhesion proteins such as COL17. The role of COL17 in cell adhesion and migration is supported by the genetic evidence derived from JEB, a disease with skin fragility and blistering. The altered epidermal patterning in COL17 deficiency might be also related to cell migration because the absence of COL17 results in Rac1 activation and aberrant directed cell migration. (Löffek et al., 2014).

Wound repair in mouse back skin requires wound contraction (Grada et al., 2018); however, the contribution of wound contraction has been regarded as minimal in the tail skin (Falanga et al., 2004). Recent studies suggest that two-thirds

of tail wound healing is due to epithelial regeneration, while wound contraction explains the remainder (Aragona et al., 2017). We believe that wound contraction does not play a major role in the slender scale phenotype in the regenerated tail skin (**Figure 15**) because of the following reasons: 1) the scale shape in the regenerated skin would become proportionally small rather than slender if the wound contraction affected this phenotype, and 2) the slender scale phenotype in the regenerated skin is rescued by K14-driven human COL17 overexpression, which might not influence wound contraction because the transgene expression is confined to the epidermis. The slender scales in *Col17a1*-/- mice most likely represent wound-related skin changes that involve the expression of wound-induced keratins in *Col17a1*-/- epidermis (**Figure 12-13**). However, the mechanisms by which wound-related skin changes affect epidermal patterning need further investigation.

Conclusion

1. COL17 is preferentially expressed in tail scale epidermis.

2. COL17 deficiency alters scale shape in the tail skin.

Transgenic rescue by the expression of human COL17 (hCOL17) under the keratin 14 (K14) promoter in *Col17a1*-/- mice reversed the slender scale phenotype

3. aPKC deregulation does not phenocopy *Col17a1*-/- scale shape.

4. Expression of wound-induced keratins is pronounced in *Col17a1*-/- tail epidermis.

5. Scale shape becomes slender after skin regeneration, and COL17 overexpression rescues the phenotype.

6. COL17 influences human skin microtopography.

Our study provides new insights into COL17 biology. *Col17a1*-/- mice have slender tail scales and are characterized by the expression of wound-induced keratins in the epidermis. In line with this, the regenerated epidermis after wounding shows slender tail scales. hCOL17 overexpression reverses the

alteration of scale shapes upon wounding. Although COL17 interacts with the aPKC complex (Watanabe et al., 2021) and helps maintain epidermal cell polarity (Liu et al., 2019; Watanabe et al., 2021), *Col17a1*-/- did not exhibit proportionally small scales as seen in aPKCλ eKO mice. This phenotypical difference indicates that the slender scale phenotype in *Col17a1*-/- mice is independent of aberrant cell polarity. These facts corroborate the role of COL17 in epidermal patterning and highlight COL17 as a therapeutic target for wound-induced skin deformations. In conclusion, our study highlights the unrecognized role of COL17 in epidermal patterning. We propose that COL17 modulation can be utilized to prevent epidermal deformation upon wounding.

Acknowledgments

I thank Dr. Hiroyuki Kiahata, Dr. Hideyuki Kosumi, and Dr. Shota Takashima for analyzing human skin patterning, Dr. Mika Watanabe, Dr. Yu Fujimura, Dr. Tomonori Hirose, Dr. Shin-Ichi Osada, Dr. Masaharu Nagayama for animal experiments, Dr. Hiroshi Shimizu and Dr. Ken Natsuga for supervising the study, and Ms. Meari Yoshida and Ms. Megumi Takehara for their technical assistance. I also thank Professor Kim B Yancey for providing K14-hCOL17 transgenic mice.

Conflict of Interest

There is no conflict of interest to disclose.

References

Aho, S., and Uitto, J. (1998). Direct interaction between the intracellular domains of bullous pemphigoid antigen 2 (BP180) and β4 integrin, hemidesmosomal components of basal keratinocytes. Biochemical and biophysical research communications *243*, 694-699.

Almeida, H.L., Jr., Goetze, F.M., Fong, K., Lai-Cheong, J., and McGrath, J. (2015). Is adermatoglyphia an additional feature of Kindler Syndrome? Anais Brasileiros de Dermatologia *90*, 592-593.

Aragona, M., Dekoninck, S., Rulands, S., Lenglez, S., Mascré, G., Simons, B.D., and Blanpain, C. (2017). Defining stem cell dynamics and migration during wound healing in mouse skin epidermis. Nature Communications *8*, 14684.

Brakebusch, C., Grose, R., Quondamatteo, F., Ramirez, A., Jorcano, J.L., Pirro, A., Svensson, M., Herken, R., Sasaki, T., and Timpl, R. (2000). Skin and hair follicle integrity is crucially dependent on β1 integrin expression on keratinocytes. The EMBO journal *19*, 3990-4003.

Braun, K.M., Niemann, C., Jensen, U.B., Sundberg, J.P., Silva-Vargas, V., and Watt, F.M. (2003). Manipulation of stem cell proliferation and lineage commitment: visualisation of label-retaining cells in wholemounts of mouse epidermis. Development *130*, 5241-5255.

Clayton, E., Doupe, D.P., Klein, A.M., Winton, D.J., Simons, B.D., and Jones, P.H. (2007). A single type of progenitor cell maintains normal epidermis. Nature *446*, 185-189.

Dekoninck, S., Hannezo, E., Sifrim, A., Miroshnikova, Y.A., Aragona, M., Malfait, M., Gargouri, S., de Neunheuser, C., Dubois, C., Voet, T., *et al.* (2020). Defining the Design Principles of Skin Epidermis Postnatal Growth. Cell *181*, 604-620.e622.

Didierjean, L., Wrench, R., and Saurat, J.H. (1983). Expression of cytoplasmic antigens linked to orthokeratosis during the

development of parakeratosis in newborn mouse tail epidermis. Differentiation *23*, 250-255.
Doupé, D.P., Klein, A.M., Simons, B.D., and Jones, P.H. (2010). The ordered architecture of murine ear epidermis is maintained by progenitor cells with random fate. Developmental Cell *18*, 317-323.
Falanga, V., Schrayer, D., Cha, J., Butmarc, J., Carson, P., Roberts, A.B., and Kim, S.J. (2004). Full‐thickness wounding of the mouse tail as a model for delayed wound healing: accelerated wound closure in Smad3 knock‐out mice. Wound repair and regeneration *12*, 320-326.
Gomez, C., Chua, W., Miremadi, A., Quist, S., Headon, D.J., and Watt, F.M. (2013). The interfollicular epidermis of adult mouse tail comprises two distinct cell lineages that are differentially regulated by Wnt, Edaradd, and Lrig1. Stem cell reports *1*, 19-27.
Goulas, S., Conder, R., and Knoblich, J.A. (2012). The Par complex and integrins direct asymmetric cell division in adult intestinal stem cells. Cell Stem Cell *11*, 529-540.
Grada, A., Mervis, J., and Falanga, V. (2018). Research techniques made simple: animal models of wound healing. Journal of Investigative Dermatology *138*, 2095-2105. e2091.
Hamill, K.J., Hopkinson, S.B., Jonkman, M.F., and Jones, J.C. (2011). Type XVII collagen regulates lamellipod stability, cell motility, and signaling to Rac1 by targeting bullous pemphigoid antigen 1e to α6β4 integrin. Journal of Biological Chemistry *286*, 26768-26780.
Has, C., Burger, B., Volz, A., Kohlhase, J., Bruckner-Tuderman, L., and Itin, P. (2010). Mild clinical phenotype of Kindler syndrome associated with late diagnosis and skin cancer. Dermatology *221*, 309-312.
Helfrich, I., Schmitz, A., Zigrino, P., Michels, C., Haase, I., le Bivic, A., Leitges, M., and Niessen, C.M. (2007). Role of aPKC isoforms and their binding partners Par3 and Par6 in

epidermal barrier formation. Journal of Investigative Dermatology *127*, 782-791.
Hopkinson, S.B., Baker, S.E., and Jones, J. (1995). Molecular genetic studies of a human epidermal autoantigen (the 180-kD bullous pemphigoid antigen/BP180): identification of functionally important sequences within the BP180 molecule and evidence for an interaction between BP180 and alpha 6 integrin. The Journal of cell biology *130*, 117-125.
Hopkinson, S.B., and Jones, J.C. (2000). The N terminus of the transmembrane protein BP180 interacts with the N-terminal domain of BP230, thereby mediating keratin cytoskeleton anchorage to the cell surface at the site of the hemidesmosome. Molecular biology of the cell *11*, 277-286.
Jones, P.H., Harper, S., and Watt, F.M. (1995). Stem cell patterning and fate in human epidermis. Cell *80*, 83-93.
Jonkman, M.F., and Pasmooij, A.M. (2009). Revertant mosaicism—patchwork in the skin. New England Journal of Medicine *360*, 1680-1682.
Kamaguchi, M., and Iwata, H. (2019). The diagnosis and blistering mechanisms of mucous membrane pemphigoid. Frontiers in Immunology *10*, 34.
Kim, S.H., Choi, H.Y., So, J.H., Kim, C.H., Ho, S.Y., Frank, M., Li, Q., and Uitto, J. (2010). Zebrafish type XVII collagen: gene structures, expression profiles, and morpholino "knock-down" phenotypes. Matrix Biology *29*, 629-637.
Knoblich, J.A. (2010). Asymmetric cell division: recent developments and their implications for tumour biology. Nature Reviews: Molecular Cell Biology *11*, 849-860.
Kobayashi, Y., Yasugahira, Y., Kitahata, H., Watanabe, M., Natsuga, K., and Nagayama, M. (2018). Interplay between epidermal stem cell dynamics and dermal deformation. npj Computational Materials *4*, 1-9.
Koster, J., Geerts, D., Favre, B., Borradori, L., and Sonnenberg, A. (2003). Analysis of the interactions between

BP180, BP230, plectin and the integrin α6β4 important for hemidesmosome assembly. Journal of cell science *116*, 387-399.
Lee, C.Y., Robinson, K.J., and Doe, C.Q. (2006). Lgl, Pins and aPKC regulate neuroblast self-renewal versus differentiation. Nature *439*, 594-598.
Lim, X., Tan, S.H., Koh, W.L., Chau, R.M., Yan, K.S., Kuo, C.J., van Amerongen, R., Klein, A.M., and Nusse, R. (2013). Interfollicular epidermal stem cells self-renew via autocrine Wnt signaling. Science *342*, 1226-1230.
Liu, N., Matsumura, H., Kato, T., Ichinose, S., Takada, A., Namiki, T., Asakawa, K., Morinaga, H., Mohri, Y., De Arcangelis, A., *et al.* (2019). Stem cell competition orchestrates skin homeostasis and ageing. Nature *568*, 344-350.
Löffek, S., Hurskainen, T., Jackow, J., Sigloch, F.C., Schilling, O., Tasanen, K., Bruckner-Tuderman, L., and Franzke, C.W. (2014). Transmembrane collagen XVII modulates integrin dependent keratinocyte migration via PI3K/Rac1 signaling. PloS One *9*, e87263.
López-Rovira, T., Silva-Vargas, V., and Watt, F.M. (2005). Different consequences of β1 integrin deletion in neonatal and adult mouse epidermis reveal a context-dependent role of integrins in regulating proliferation, differentiation, and intercellular communication. Journal of Investigative Dermatology *125*, 1215-1227.
Mascré, G., Dekoninck, S., Drogat, B., Youssef, K.K., Broheé, S., Sotiropoulou, P.A., Simons, B.D., and Blanpain, C. (2012). Distinct contribution of stem and progenitor cells to epidermal maintenance. Nature *489*, 257-262.
Matsumura, H., Mohri, Y., Binh, N.T., Morinaga, H., Fukuda, M., Ito, M., Kurata, S., Hoeijmakers, J., and Nishimura, E.K. (2016). Hair follicle aging is driven by transepidermal elimination of stem cells via COL17A1 proteolysis. Science *351*.
McGrath, J.A., Gatalica, B., Christiano, A.M., Owaribe, K., McMillan, J.R., Eady, R.A., and Uitto, J. (1995). Mutations in the 180-kD bullous pemphigoid antigen (BPAG2), a hemidesmosomal

transmembrane collagen (COL17A1), in generalized atrophic benign epidermolysis bullosa. Nature genetics *11*, 83-86.
Moreci, R.S., and Lechler, T. (2020). Epidermal structure and differentiation. Current Biology *30*, R144-R149.
Morrow, A., Underwood, J., Seldin, L., Hinnant, T., and Lechler, T. (2019). Regulated spindle orientation buffers tissue growth in the epidermis. Elife *8*, e48482.
Muroyama, A., and Lechler, T. (2012). Polarity and stratification of the epidermis. Seminars in Cell & Developmental Biology *23*, 890-896.
Nakamura, H., Sawamura, D., Goto, M., Nakamura, H., Kida, M., Ariga, T., Sakiyama, Y., Tomizawa, K., Mitsui, H., and Tamaki, K. (2006). Analysis of the COL17A1 in non-Herlitz junctional epidermolysis bullosa and amelogenesis imperfecta. International journal of molecular medicine *18*, 333-337.
Natsuga, K. (2014). Epidermal barriers. Cold Spring Harbor perspectives in medicine *4*, a018218.
Natsuga, K., Nishie, W., Nishimura, M., Shinkuma, S., Watanabe, M., Izumi, K., Nakamura, H., Hirako, Y., and Shimizu, H. (2017). Loss of interaction between plectin and type XVII collagen results in epidermolysis bullosa simplex. Human mutation *38*, 1666-1670.
Natsuga, K., Watanabe, M., Nishie, W., and Shimizu, H. (2019). Life before and beyond blistering: the role of collagen XVII in epidermal physiology. Experimental Dermatology *28*, 1135-1141.
Niculescu, C., Ganguli-Indra, G., Pfister, V., Dupé, V., Messaddeq, N., De Arcangelis, A., and Georges-Labouesse, E. (2011). Conditional ablation of integrin alpha-6 in mouse epidermis leads to skin fragility and inflammation. European journal of cell biology *90*, 270-277.
Niessen, M.T., Iden, S., and Niessen, C.M. (2012). The in vivo function of mammalian cell and tissue polarity regulators–how to shape and maintain the epidermal barrier. Journal of cell science *125*, 3501-3510.

Niessen, M.T., Scott, J., Zielinski, J.G., Vorhagen, S., Sotiropoulou, P.A., Blanpain, C., Leitges, M., and Niessen, C.M. (2013). aPKCλ controls epidermal homeostasis and stem cell fate through regulation of division orientation. Journal of Cell Biology *202*, 887-900.
Nishie, W., Kiritsi, D., Nyström, A., Hofmann, S.C., and Bruckner-Tuderman, L. (2011). Dynamic interactions of epidermal collagen XVII with the extracellular matrix: laminin 332 as a major binding partner. The American journal of pathology *179*, 829-837.
Nishie, W., Sawamura, D., Goto, M., Ito, K., Shibaki, A., McMillan, J.R., Sakai, K., Nakamura, H., Olasz, E., and Yancey, K.B. (2007). Humanization of autoantigen. Nature medicine *13*, 378-383.
Nishimura, M., Nishie, W., Shirafuji, Y., Shinkuma, S., Natsuga, K., Nakamura, H., Sawamura, D., Iwatsuki, K., and Shimizu, H. (2016). Extracellular cleavage of collagen XVII is essential for correct cutaneous basement membrane formation. Human molecular genetics *25*, 328-339.
Noguchi, N., Hirose, T., Suzuki, T., Kagaya, M., Chida, K., Ohno, S., Manabe, M., and Osada, S.-I. (2019). Atypical protein kinase C isoforms differentially regulate directional keratinocyte migration during wound healing. Journal of Dermatological Science *93*, 101-108.
Nomura, T. (2020). Recombination-induced revertant mosaicism in ichthyosis with confetti and loricrin keratoderma. Journal of Dermatological Science *97*, 94-100.
Osada, S.-I., Minematsu, N., Oda, F., Akimoto, K., Kawana, S., and Ohno, S. (2015). Atypical protein kinase C isoform, aPKCλ, is essential for maintaining hair follicle stem cell quiescence. Journal of Investigative Dermatology *135*, 2584-2592.
Poulson, N.D., and Lechler, T. (2012). Asymmetric cell divisions in the epidermis. International Review of Cell and Molecular Biology *295*, 199-232.

Sada, A., Jacob, F., Leung, E., Wang, S., White, B.S., Shalloway, D., and Tumbar, T. (2016). Defining the cellular lineage hierarchy in the interfollicular epidermis of adult skin. Nature cell biology *18*, 619-631.
Sánchez-Danés, A., Hannezo, E., Larsimont, J.C., Liagre, M., Youssef, K.K., Simons, B.D., and Blanpain, C. (2016). Defining the clonal dynamics leading to mouse skin tumour initiation. Nature *536*, 298-303.
Schaapveld, R.Q., Borradori, L., Geerts, D., Van Leusden, M.R., Kuikman, I., Nievers, M.G., Niessen, C.M., Steenbergen, R.D., Snijders, P.J., and Sonnenberg, A. (1998). Hemidesmosome formation is initiated by the β4 integrin subunit, requires complex formation of β4 and HD1/plectin, and involves a direct interaction between β4 and the bullous pemphigoid antigen 180. The Journal of cell biology *142*, 271-284.
Schweizer, J., and Marks, F. (1977). A developmental study of the distribution and frequency of Langerhans cells in relation to formation of patterning in mouse tail epidermis. Journal of Investigative Dermatology *69*, 198-204.
Simons, M., and Mlodzik, M. (2008). Planar cell polarity signaling: from fly development to human disease. Annual Review of Genetics *42*, 517-540.
Stouthamer, A., Nieboer, C., Van der Waal, R., and Jonkman, M. (2001). Normal expression of the 19‐DEJ‐1 epitope in two siblings with late‐onset junctional epidermolysis bullosa. British Journal of Dermatology *144*, 1054-1057.
Tanimura, S., Tadokoro, Y., Inomata, K., Binh, N.T., Nishie, W., Yamazaki, S., Nakauchi, H., Tanaka, Y., McMillan, J.R., and Sawamura, D. (2011). Hair follicle stem cells provide a functional niche for melanocyte stem cells. Cell stem cell *8*, 177-187.
Tasanen, K., Tunggal, L., Chometon, G., Bruckner-Tuderman, L., and Aumailley, M. (2004). Keratinocytes from patients lacking collagen XVII display a migratory phenotype. The American journal of pathology *164*, 2027-2038.

Tellkamp, F., Vorhagen, S., and Niessen, C.M. (2014). Epidermal polarity genes in health and disease. Cold Spring Harbor perspectives in medicine *4*, a015255.
Vorhagen, S., and Niessen, C.M. (2014). Mammalian aPKC/Par polarity complex mediated regulation of epithelial division orientation and cell fate. Experimental cell research *328*, 296-302.
Wang, S., Drummond, M.L., Guerrero-Juarez, C.F., Tarapore, E., MacLean, A.L., Stabell, A.R., Wu, S.C., Gutierrez, G., That, B.T., and Benavente, C.A. (2020). Single cell transcriptomics of human epidermis identifies basal stem cell transition states. Nature communications *11*, 1-14.
Watanabe, M., Kosumi, H., Osada, S.I., Takashima, S., Wang, Y.A., Nishie, W., Oikawa, T., Hirose, T., Shimizu, H., and Natsuga, K. (2021). Type XVII collagen interacts with the aPKC-PAR complex and maintains epidermal cell polarity. Experimental Dermatology *30*, 62-67.
Watanabe, M., Natsuga, K., Nishie, W., Kobayashi, Y., Donati, G., Suzuki, S., Fujimura, Y., Tsukiyama, T., Ujiie, H., and Shinkuma, S. (2017). Type XVII collagen coordinates proliferation in the interfollicular epidermis. Elife *6*, e26635.
Watt, F.M., and Fujiwara, H. (2011). Cell-extracellular matrix interactions in normal and diseased skin. Cold Spring Harbor Perspectives in Biology *3*, a005124.
Yuen, W.Y., and Jonkman, M.F. (2011). Risk of squamous cell carcinoma in junctional epidermolysis bullosa, non-Herlitz type: report of 7 cases and a review of the literature. Journal of the American Academy of Dermatology *65*, 780-789.